

Annual Review
2020

Molecular Photoscience
Research Center

Kobe University

Preface

This annual review provides a summary of the research activity of Molecular Photoscience Research Center for the 2020 academic year. We are further promoting advanced research and international collaboration on molecular photoscience and related topics. Any constructive comments and questions, and any suggestion for collaboration research are welcome.

Since 2017 we have been running joint usage/research project on molecular science in the terahertz frequency region, which is open to domestic universities and research institutes. In this year 36 joint research projects were accepted, and the research area spans from solid state physics, biophysics, solution chemistry, polymer science, photochemistry, theoretical physics and chemistry, so on. In this year we also started a series of seminars for the four research areas (solar energy conversion, high-resolution spectroscopy in gas phase, spin material physics, and hydration of soft matter) in the terahertz molecular science. The research center will continue to make efforts to push forward international and domestic collaborative research.

April, 2021

Keisuke Tominaga

Director of Molecular Photoscience Research Center,
Kobe University



Contents

Members	5
Research Activities	
Laser Molecular Photoscience Laboratory	6
Terahertz Molecular Chemistry Laboratory	16
Terahertz Material Physics Laboratory	24
Original Papers	37
Invited Talks	40
Presentation at Conferences (International and domestic)	41
Presentation by Graduate Students and Postdocs	43
Books	46
Other Publications	47
Lectures to Public	48
Awards	49
Conference Organization	50
Seminars	51

Research Activity

I. Laser Molecular Photoscience Laboratory

I-A. SPIN INTERACTIONS STUDIED BY TIME RESOLVED MAGNETIC RESONANCE SPECTROSCOPY

In the natural photosynthesis, the organic solar cells and the photocatalysis, transient radical species or carriers are immediately generated by the light-induced chemical reactions for the photo-energy conversion, providing essential sources of the living energies. However, it has been unclear how those transient molecules are initially interacting each other before the carrier-conductions or charge-dissociation take place. In our group, we are developing experimental methodologies to determine molecular positions, orbital orientations and orbital overlap (electronic coupling) in the initially generated radical-pairs, multiexcitons, and electron-hole pairs in the photoactive proteins, in the solar cells, and in the photocatalysis on the basis of the transient electron paramagnetic resonance (EPR) method. We have clarified several fundamental mechanisms of the energy-conversions in semiconductor nanoparticles, singlet-fission materials and in the polymer systems.

Fast T-Type Photochromism of Colloidal Cu-Doped ZnS Nanocrystals

Y. Han¹, M. Hamada, I. Chang², K. Hyeon-Deuk², Y. Kobori, Y. Kobayashi¹

¹Ritsumeikan University

²Kyoto University

(*J. Am. Chem. Soc.*, 2021)

This paper reports on durable and nearly temperature-independent (at 298–328 K) T-type photochromism of colloidal Cu-doped ZnS nanocrystals (NCs). The color of Cu-doped ZnS NC powder changes from pale yellow to dark gray by UV light irradiation, and the color changes back to pale yellow on a time scale of several tens of seconds to minutes after stopping the light irradiation, while the decoloration reaction is accelerated to submillisecond in solutions. This decoloration reaction is much faster than those of conventional inorganic photochromic materials. The

origin of the reversible photoinduced coloration is revealed to be a strong optical transition involving a delocalized surface hole which survives over a minute after escaping from intraparticle carrier recombination due to electron-hopping dissociation. ZnS NCs can be easily prepared in a water-mediated one-pot synthesis and are less toxic. Therefore, they are promising for large-scale photochromic applications such as windows and building materials in addition to conventional photochromic applications. Moreover, the present study demonstrates the importance of excited carrier dynamics and trap depths, resulting in coloration over minutes not only for photochromic nanomaterials but also for various advanced photofunctional materials, such as long persistent luminescent materials and photocatalytic nanomaterials.

Geometries and Terahertz Motions Driving Dissociations via the Intramolecular Singlet Quintet Multiexcitons and Ultimate Triplet–Triplet Fissions

Y. Kobori, M. Fuki, S. Nakamura¹, T. Hasobe¹

¹Keio University

(J. Phys. Chem. B, 2020)

Importance of vibronic effects has been highlighted for the singlet-fission (SF) that converts one high-energy singlet exciton into doubled triplet excitons, as strongly coupled multiexcitons. However, molecular mechanisms of spin conversion processes and ultimate decouplings in the multiexcitons are poorly understood. We have analyzed geometries and exchange couplings (singlet–quintet energy gaps: $6J$) of the photoinduced multiexcitons in the pentacene dimers bridged by a phenylene at ortho and meta positions [denoted as o-(Pc)₂ and m-(Pc)₂] by

simulations of the time-resolved electron paramagnetic resonance spectra. We clarified that terahertz molecular conformation dynamics play roles on the spin conversion from the singlet strongly coupled multiexcitons ¹(TT) to the quintet multiexcitons ⁵(TT) and on the intramolecular decouplings in the $6J$ to form spin correlated triplet pairs (T+T). The strongly coupled ⁵(TT) multiexcitons are revealed to possess entirely planar conformations stabilized by mutually delocalized spin distributions, while the intramolecular decoupled spin-correlated triplet pairs generated at 1 μs are also stabilized by distorted conformations resulting in two separately localized biradical characters.

Photon-to-Energy Conversion Mechanisms Revealed by Quantum Effects on Electron Spin Polarization

Y. Kobori

(The Japanese Photochemistry Association Award 2019 Lecture, Invited)

Despite importance of elucidating generation mechanisms of photoinduced excitons and charges for developments of the efficient photon-to-energy conversion systems, it has been quite difficult to characterize molecular geometries, electronic couplings and the mobilities at the photoinduced initial charge-separations (CS) and the singlet-fissions (SF) for heterogeneous molecular environments in protein complexes, bulk heterojunction (BHJ) interfaces between the electron donor acceptor domains in the photoactive layers of the organic solar cells (OSC), and in the disordered thin films. We have employed the time-resolved electron paramagnetic resonance (TREPR) methods to characterize several electron spin polarizations (ESP) [1-14] of the photoinduced

intermediate states to characterize the geometries, electronic couplings of spin-correlated paramagnetic pairs by determinations and extractions of the anisotropic magnetic interactions and the exchange-couplings including the SF systems [1,3]. In particular, a novel tool of mapping the ESPs to space directions [2,4] has been demonstrated to be powerful for understanding how several nuclear motions contribute to the intermediate geometries and their mobilities for light-induced primary energy conversion processes (Fig. 1). [1-3]

It has been desired to understand the primary photon-to-energy conversions processes in the plant photosynthesis, OSC thin films and the artificial photosynthesis for developments of the next-generation devices that enable us to convert the solar energies to the chemical reactions more efficiently. For these, it is important to elucidate the roles played by molecular geometries and motions on the electronic interactions of photoinduced primary processes in CS and the singlet-fissions (SF) in several organic systems.

In 1987, Closs, Forbes and Norris proposed a mechanism to interpret antiphase TREPR spectra generated in radical pairs by photoreactions in confined molecular systems; i.e. the spin correlated radical pair (SCRCP) model. (*J. Phys. Chem.* 1987, 91, 3592.) Since then, the SCRCP models have long been utilized on several reaction systems in biology and in material science to interpret the magnetic interactions and dynamics of the key intermediates.

We have extended the SCRCP model to the rigorous scientific analysis tools establishing the electron spin polarization transfer (ESPT) mechanism including the spin coherences and decoherences through spin-polarized higher spin-multiplicities in a wide variety of systems [1,2,10,11,13]. This ESPT model has strong impact to distinguish the anisotropic and isotropic effects on ESP mainly by the combinations of magnetophotoselection detections with which the polarized excitation lights are utilized to unambiguously determine the molecular geometries and the electronic couplings in the reaction intermediates. [2,4,5,12] This enabled us for the first time to experimentally understand how the molecular conformations and the vibrations contribute to the electronic interactions on the energy conversion processes in several environments. [1-14] Furthermore, we have achieved major breakthroughs on unveiling the reaction mechanisms by mapping the anisotropic ESP to all possible magnetic field directions to highlight clear 3D-visualizations of the geometries of the reaction intermediates even in the highly disordered and the heterogeneous environments (Fig. 1). This electron spin polarization imaging method has recently demonstrated impacts of both of the intramolecular high-frequency stretching vibrations and the phonons on the efficient electron-hole dissociations at the BHJ interfaces in OCS.[2]

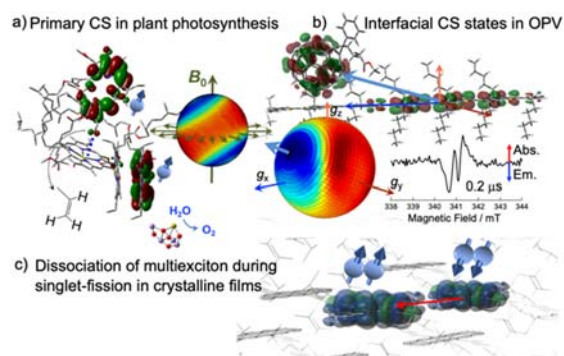


Figure 1. Geometries of the intermediate CS states in plant PSII membrane [4] in a), and OCS [2] in b), and the multiexcitons [1] in c) as revealed by characterizing the anisotropic ESP by using the TREPR method.

References:

- [1] S. Matsuda, S. Oyama, Y. Kobori, *Chem. Sci.* 2020, 11, 2934.
- [2] Y. Kobori, T. Ako, S. Oyama, T. Tachikawa, K. Marumoto. *J. Phys. Chem. C* 2019, 123, 13472.
- [3] Y. Matsui, S. Kawaoka, H. Nagashima, T. Nakagawa, N. Okamura, T. Ogaki, E. Ohta, S. Akimoto, A. Sato-Tomita, S. Yagi, Y. Kobori, H. Ikeda, *J. Phys. Chem. C* 2019, 123, 18813.
- [4] M. Hasegawa, H. Nagashima, R. Minobe, T. Tachikawa, H. Mino, Y. Kobori, *J. Phys. Chem. Lett.* 2017, 8, 1179.
- [5] M. Fuki, H. Murai, T. Tachikawa, Y. Kobori, *J. Phys. Chem. B* 2016, 120, 4365.
- [6] T. Miura, R. Tao, S. Shibata, T. Umeyama, T. Tachikawa, H. Imahori, Y. Kobori. *J. Am. Chem. Soc.* 2016, 138, 5879.
- [7] Y. Kobori, T. Miura, J. R. Norris, *J. Phys. Chem. Lett.* 2015, 6, 113. (Perspective)
- [8] Y. Kobori, N. Ponomarenko, J. R. Norris, *J. Phys. Chem. C* 2015, 119, 8078.
- [9] T. Miura, M. Aikawa, Y. Kobori, *J. Phys. Chem. Lett.*, 2014, 5, 30.

- [10] Y. Kobori, R. Noji, S. Tsuganezawa, *J. Phys. Chem. C* 2013, 117, 1589.
- [11] R. Carmieli, A. Smeigh, S. M. Conron, A. Thazhathveetil, M. Fuki, Y. Kobori, F. Lewis, M. Wasielewski *J. Am. Chem. Soc.* 2012, 134, 11251.
- [12] Y. Kobori, M. Fuki *J. Am. Chem. Soc.* 2011, 133, 16770.
- [13] Y. Kobori, M. Fuki, H. Murai, *J. Phys. Chem. B* 2010, 114, 14621.
- [14] Y. Kobori, Y. Shibano, T. Endo, H. Tsuji, H. Murai, K. Tamao, *J. Am. Chem. Soc.* 2009, 131, 1624.

I-B. SINGLE-MOLECULE STUDIES ON PHOTO-ENERGY CONVERSION PROCESSES

To design a more efficient solar energy conversion system (light energy to electrical or chemical energy), it is important to reveal and understand the mechanisms of various chemical reactions at heterogeneous interfaces.

We have investigated the photochemical and photophysical processes occurring on a variety of light energy conversion systems such as photocatalysis and solar cells using advanced single-molecule, single-particle spectroscopy techniques and gain new insights related to spatial and temporal heterogeneities in reactions and structures, which are always masked by ensemble averaging.

Ultra-Narrow Depletion Layers in Hematite Mesocrystal-Based Photoanode for Boosting Multihole Water Oxidation

Zhujun Zhang, Hiroki Nagashima and Takashi Tachikawa

(*Angew. Chem. Int. Ed.*, 2020)

Photoelectrochemical (PEC) water splitting allows for the direct conversion of solar energy to clean and renewable energy sources such as H₂ gas, providing an attractive solution to energy and environmental issues. Hematite (α -Fe₂O₃) is an ideal semiconductor for solar water splitting but shows low efficiency due to the significant charge recombination. Mesocrystals (MCs) are superstructures of combined nanoparticles with same crystal orientation. In this study, Ti-modified hematite MC superstructures assembled from highly oriented tiny nanoparticle subunits with sizes of ca. 5 nm were developed to achieve the highest photocurrent density (4.3 mA cm⁻² at 1.23 V vs. RHE) under back illumination (Figure 1). The rich interfacial

oxygen vacancies yield an exceedingly high carrier density of 4.1×10^{21} cm⁻³ for super bulk conductivity in the electrode and a large proportion of ultra-narrow depletion layers (<1 nm) inside the mesoporous film. The deep band bending on the surface should provide a great enough potential gradient to drive the separation of photogenerated electrons and holes and, thus, effectively suppress bulk recombination, as evidenced by the very small internal resistances analyzed by electrochemical impedance spectroscopy. We further employed photoconductive atomic force microscopy to elucidate structure-correlated electrical transport properties inherent in individual MC particles with nanoscale resolution. To unravel the water oxidation mechanism, the temperature dependence of photocurrent generation from the optimized Ti-modified hematite MC photoanode was studied. A very low activation energy ($E_a = 44$ meV) obtained from Arrhenius-type plots of $\ln J$ vs. $1/T$, where J is the current density, may suggest third-order-

like water oxidation kinetics. Our study provides an attractive strategy based on interfacial defect engineering for improving the PEC performance of metal oxide semiconductors.

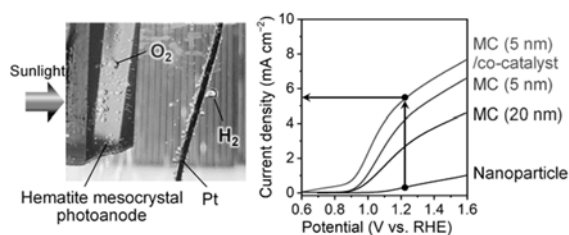


Figure 1. Solar-driven water splitting (left) and performance (right) of hematite photoanodes.

In Situ Exploration of the Structural Transition during Morphology and Efficiency-Conserving Halide Exchange on a Single Perovskite Nanocrystal

Izuru Karimata and Takashi Tachikawa

(*Angew. Chem. Int. Ed.*, 2020)

Metal halide perovskites (such as MAPbI₃, MA = CH₃NH₃⁺) have recently attracted much attention as light absorbers in photovoltaic cells and as promising materials for optoelectronic applications including lasers and light emitting diodes. In this study, transformation from red-emitting metal halide perovskite MAPbI₃ nanocrystals (NCs) to green-emitting MA₃PbBr₃ NCs was achieved without significant morphological changes and loss of photoluminescence (PL) efficiency via a controlled halide exchange reaction. Figure 1 shows the PL spectra of MAPbI₃ NCs with a mean size of ca. 90 nm during halide exchange with Br⁻ using a custom-made flow reactor. The controlled flow of octylammonium bromide solution caused a continuous peak shift from 770 nm to 620 nm accompanied by an initial increase, and a subsequent decrease in the PL intensity. After a while, a detectable peak appeared at approximately 550 nm, and then became more intense over time and eventually shifted to 530 nm. In situ single-particle PL

imaging along with detailed structural and elemental characterizations revealed that sudden cooperative transitions between two light-emitting states via intermediate dark states with >100 s durations during halide exchange originate from two distinct defect-mediated reconstruction processes with different activation energies (0.072 and 0.40 eV), leading to an isokinetic temperature of ca. 314 K, across a solid-state miscibility gap between the I- and Br-rich phases inside a single NC. Our single-particle approach for controlling and evaluating the rate-limiting processes of ion exchange on nanostructures will help to improve device performance and will open new avenues for extending the applications of halide perovskite NCs.

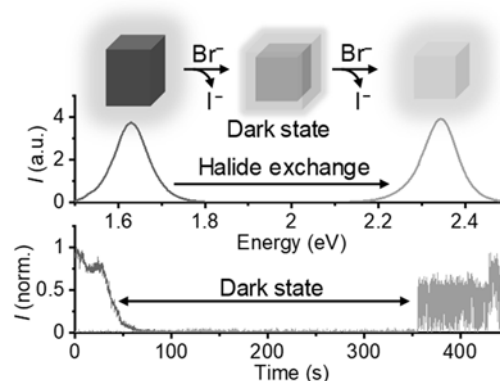


Figure 1. Halide exchange reaction on single perovskite nanoparticles.

Unraveling Hidden Correlations between Molecular Diffusivity and Reactivity in Ruthenium Complex-Modified Mesoporous Silica

Tatsuya Watase, Minoru Sohmiya,¹ Zhujun Zhang, Yasuhiro Kobori and Takashi Tachikawa

¹Seikei University

(*J. Phys. Chem. C*, 2020)

Mesoporous silicas (MPSs) are widely used as host materials for applications involving molecular sorption, separation, storage, and (photo)catalysis. Herein, we report single-molecule, single-particle approaches for exploring molecular diffusion and photochemical reactions in ruthenium (Ru) complex-modified MPS particles. Single-particle fluorescence recovery after photobleaching (FRAP) experiments revealed that Ru complexes are mobile in MPS with diffusion coefficients in the range of 10^0 – 10^2 nm² s⁻¹, which vary among the particles and locations, and their diffusivity decreases with increasing amount of sulfonated phenyl groups, which act as adsorption sites for positively charged Ru complexes, on the silica surface. Next, we focused on the detection of •OH over single Ru dye-modified MPS particles by utilizing TIRF microscopy. Figure 1 shows the fluorescence images captured for a single Ru dye-

modified MPS particle in phosphate buffer before and after the addition of APF under 488 nm laser irradiation. The burst spots are likely located near the center of the particle (shown as a broken circle). This result suggests that a part of the products generated near the outer surface escaped, again supporting our conclusion that a series of reactions take place within a single particle. By combining the above methods, a positive correlation between molecular diffusivity and reactivity was validated, suggesting the importance of well-ordered nanochannels with optimized pore diameters and adequate environments for efficient heterogeneous (photo)catalysis.

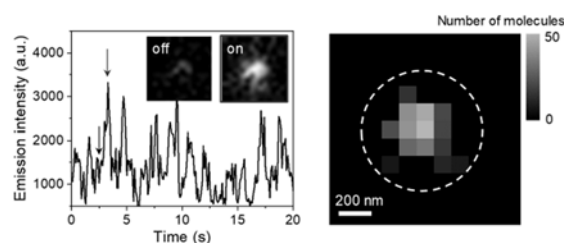


Figure 1. Intensity trajectory observed during 488 nm laser excitation of a single Ru dye-modified MPS particle in the presence of APF (left). Spatial distribution of the locations of fluorescein molecules (right).

I-C. HIGH-RESOLUTION SPECTROSCOPY OF POLIATOMIC MOLECULES

Doppler-free high-resolution spectroscopy is a powerful tool for studying the structure and dynamics of excited polyatomic molecules in detail and unambiguously. Single-mode auto-scan laser systems for the UV-Visible-NIR region, the absolute wavenumber measurement system, and Doppler-free high-resolution spectroscopic measurement systems have been constructed to investigate the excited molecules.

High-resolution and high-precision measurement of spectral lines enables to observe rotationally-resolved electronic transition, then it is expected to find the excited state dynamics such as internal conversion (IC), intersystem crossing (ISC), and intramolecular vibrational redistribution (IVR) through the deviations in spectral line positions, intensity anomalies, and the changes of spectral linewidth. We have observed the high-

resolution spectrum and the Zeeman effects of the π - π^* transition of several aromatic molecules such as benzene, naphthalene, anthracene, etc. and these molecular constants were determined in high-accuracy.

Recently, we extended our observation to the molecules with large amplitude motion such as acetaldehyde and trans-stilbene.

Ultrahigh-resolution Spectroscopy of acetaldehyde: Torsion-inversion-rotation interaction in the excited state

Kosuke Nakajima, Akira Shimizu, Shunji Kasahara, Masatoshi, Misono, Masaaki Baba

(5th Asian Workshop on Molecular Spectroscopy, 2021)

Acetaldehyde is one of a prototype for study of the methyl torsion (internal rotation), which is the typical large amplitude motion. According to the reported study, the tunneling splitting due to the torsional barrier was found. In the S_1 state, the aldehyde-hydrogen inversion belong to the large amplitude motion because the planer conformation changes to the pyramidal conformation involving the aldehyde-hydrogen distortion. Therefore, acetaldehyde in the $S_1(n\pi^*)$ state has these two large amplitude motions unlike the S_0 state. These two large amplitude motions correspond to the vibrational mode of ν_{15} and ν_{14} , respectively. In the S_1 state, it is necessary to consider the interaction between the overall rotation and these two large amplitude motions, and the rotation structure is more complicated than in the S_0 state. Several studies on $S_1(n\pi^*) \leftarrow S_0$ transition have been reported. The vibronic spectra ($S_1(n\pi^*) \leftarrow S_0$) under jet-cooled condition were observed by Baba *et al.* and Noble *et al.* [1-2]. And, rotationally resolved spectra were observed using a pulsed amplified CW laser [3-5] because their intensity is weak.

In this work, rotationally-resolved high-resolution fluorescence excitation spectra have been observed by improvement of detection efficiency, instead of enhancement of laser power by pulsed amplifier. Then, the observed spectra were higher resolution than the reported spectra. The parts of observed spectra are shown in Fig. 1. The typical linewidth of observed spectra was about 40 MHz. The observed spectra around 30117 cm^{-1} (a) and 30380 cm^{-1} (b) correspond to $14_0^{0+}15_0^2$ and $14_0^{0\pm}15_0^4$ band, respectively. In comparison with the torsional barrier energy, the 15^2 vibrational level in the S_1 state is lower energy, on the other hand, 15^4 vibrational level is higher energy.

We are trying to analyze the observed spectra based on consideration of the interaction among the overall rotation and these two large amplitude motions, and then determine the rotational constant of the S_1 state which is physically meaning.

References:

- 1) M. Noble, E. K. C. Lee, *J. Chem. Phys.* **81**, 1632, (1984).
- 2) M. Baba, I. Hanazaki, U. Nagashima, *J. Chem. Phys.* **82**, 3938, (1985).
- 3) H. Liu, E. C. Lim, C. Muñoz-Caro, A. Niño, R. H. Judge, D. C. Moule, *J. Mol. Spectrosc.* **175**, 172, (1996).
- 4) Y.-C. Chou, C.-L. Huang, I.-C. Chen, C.-K. Ni, A. H. Kung, *J. Chem. Phys.* **115**, 5089, (2001).

5) E. Jalviste, G. Berden, M. Drabbels, A. M. Wodtke, *J. Chem. Phys.* **114**, 8316 (2001).

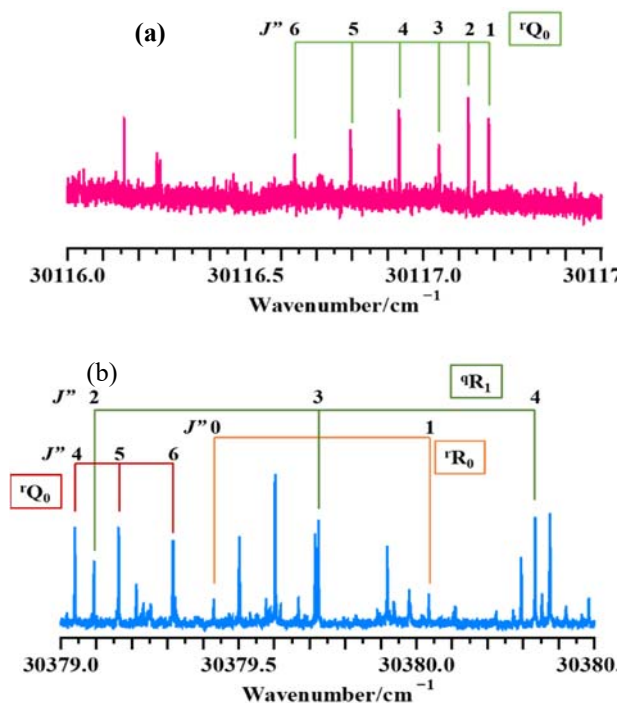


Figure 1. A part of ultrahigh-resolution fluorescence excitation spectra of acetaldehyde of $S_1(n\pi^*) \leftarrow S_0$ transition. (a) $14_0^{0+}15_0^2$ band. (b) $14_0^{0+}15_0^4$ band. Intensity of the lower spectra (b) is 1/3 scale of that of the upper spectra (a).

Ultrahigh-resolution spectroscopy of *trans*-stilbene: nonplanar structure in the ground state

Akira Shimizu, Kosuke Nakajima, Shunji Kasahara, Naofumi Nakayama, Masatoshi, Misono, Masaaki Baba

(5th Asian Workshop on Molecular Spectroscopy, 2021)

The photoisomerization of stilbene is an important model for chemical reaction dynamics. Many groups studied reaction dynamics of *trans*-stilbene in gaseous phase¹⁾⁻³⁾ by using spectroscopic techniques.

High-resolution spectra of *trans*-stilbene S_1 - S_0 transition were observed by Leo Meerts et.al³⁾. They concluded the structure of *trans*-stilbene in S_0 state is planar from the obtained rotational constants. In order to consider the structure and potential energy surface of *trans*-stilbene correctly, we applied the high-

resolution laser spectroscopy and theoretical calculation by Gaussian program.

High-resolution fluorescence excitation spectra of the 0_0^0 band and several vibronic bands in S_1 - S_0 transition of *trans*-stilbene have been observed by crossing a single mode UV laser beam perpendicular to a molecular beam. Figure 1 shows the observed high-resolution spectra of 0_0^0 band of *trans*-stilbene S_1 - S_0 transition. Rotational structure was found in the observed spectra. However, each rotational line was not resolved completely due to the lifetime broadening. The fluorescence life time of S_1 state is reported as 2.7 ns^{1,2)}.

The observed spectra of 0_0^0 band and several vibronic bands were *a*-type band. For the 0_0^0 band, we determined the rotational constants, linewidth and rotational temperature by comparison between the

observed spectrum and calculated spectrum by using PGOPHER program. From the obtained rotational constants and inertial defect, it was found S_0 structure is not planar. To confirm this result, we calculate the molecular structure based on DFT calculation, it suggested phenyl rings are twisted almost 5 degree.

References:

- 1) T. J. Majors, U. Even, and J. Jortner, *J. Chem. Phys.* **81**, 2330 (1984).
- 2) J. A. Syage, P. M. Felker, and A. H. Zewail, *J. Chem. Phys.* **81**, 4706 (1984).
- 3) B. B. Champagne, J. F. Pfanstiel, D. F. Plusquellic, D. W. Pratt, W. M. van Herpen, and W. L. Meerts, *J. Phys. Chem.* **94**, 6 (1990).

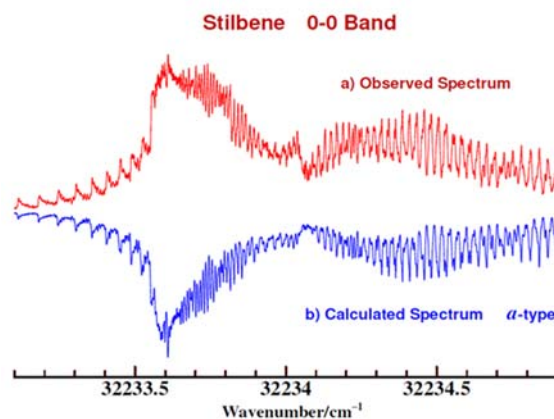


Figure 1. High-resolution spectra of *trans*-stilbene 0_0^0 band, a) Observed Spectrum, b) Calculated Spectrum.

I-D. HIGH-RESOLUTION SPECTROSCOPY OF NO_2 AND NO_3 RADICAL

Nitrogen dioxide NO_2 and nitrate radical NO_3 have been known as an important intermediate in chemical reaction in the atmosphere. These radicals are the prototype molecules to understand vibronic interaction as followings; the Renner-Teller effect for NO_2 , and the Jahn-Teller (JT) and pseudo Jahn-Teller (PJT) effects for NO_3 . Optically allowed transitions have been observed as strong absorption and LIF excitation spectra by several research groups. For NO_2 radical, hyperfine splittings are observed in high-resolution spectrum, and the magnitude of the hyperfine interaction constants suggest the state mixing between the electronic excited state and the ground state through the vibronic interaction. Recently, we reported the hyperfine-resolved high-resolution spectrum NO_2 A-X system for the 14500-16800 cm^{-1} region.

Hyperfine-resolved high-resolution laser spectroscopy of $^{14}\text{NO}_2$ radical in the 15885 cm^{-1} energy region

Kohei Tada and Shunji Kasahara

(*J. Mol. Struct.*, 2020)

Hyperfine-resolved high-resolution fluorescence excitation spectrum of the $\tilde{A}^2B_2 \leftarrow \tilde{X}^2A_1$ transition of $^{14}\text{NO}_2$ radical in the 15870 – 15900 cm^{-1} energy region was observed, by crossing a jet-cooled

molecular beam and an output of a single-mode dye laser at the right angles. We obtained the rotational assignments up to $N' = 11$ for the $K_a = 0$ series and those up to $N' = 7$ for the $K_a = 1$ series by analyzing the observed hyperfine structures and employing the combination differences, and determined the molecular constants of the upper vibronic level. Most of the Fermi contact interaction constants of the rotational levels of the upper vibronic level was found

to range from 0.002 cm^{-1} to 0.004 cm^{-1} . The ($K_a' = 0$, $N' = 3$, $J' = 3.5$) level was found to be strongly perturbed, and we recognized some perturbers in the vicinity of the main rotational level. We concluded that the most plausible candidate of the perturbers in this region is the vibronic levels of the \tilde{A}^2B_2 electronic state.

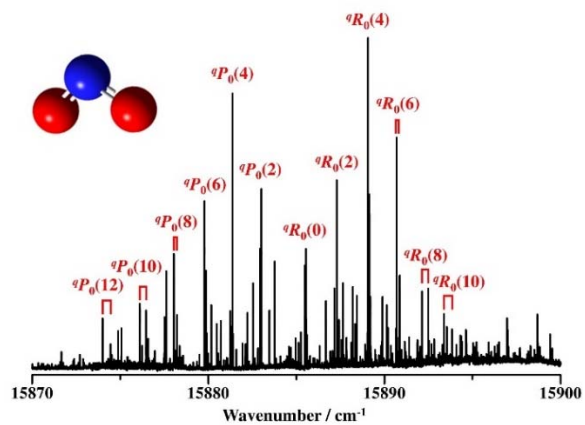


Figure 1. The fluorescence excitation spectrum in $15870\text{--}15900\text{ cm}^{-1}$ energy region. The rotational temperature was estimated to 25 K.

II. Terahertz Molecular Chemistry Laboratory

II-A. LIQUID DYNAMICS STUDIED BY NONLINEAR INFRARED SPECTROSCOPY

Molecular dynamics in liquids are strongly affected by the nature of intermolecular interactions. It is greatly important to obtain the molecular description on relation between the dynamics and interactions in liquids in order to elucidate the solvent dynamical effect on chemical reactions. In solutions, a vibrational frequency of solute molecule is sensitive to changes of the solvent environment. Especially, in aqueous solution, hydrogen-bond making and breaking processes play an important role in the dynamics of water molecules surrounding the solute. Fluctuations of the vibrational transition energies, which are characterized by time correlation functions of the frequency fluctuations, are very sensitive to the dynamics of surrounding environments. Vibrational energy relaxation is also affected by short-range solvent-oscillator interaction.

Furthermore, orientational relaxation reflects microscopic viscosity around the oscillator. In recent years, a great deal of effort has been devoted to investigate solute-solvent interactions with infrared (IR) nonlinear spectroscopy such as two-dimensional IR (2D-IR) spectroscopy and pump-probe spectroscopy. 2D-IR spectroscopy is a powerful tool to obtain microscopic information in solution such as ultrafast solvent dynamics and local structure of solvent by probing the vibrational frequency fluctuations. By polarization-sensitive pump-probe spectroscopy in the IR region we can study vibrational energy relaxation and orientational relaxation.

Hydrogen Bond Dynamics of 9-Fluorenone Derivatives in Water Studied by Two-Dimensional Infrared Spectroscopy

Yuki Fujii, Kaoru Ohta, and Keisuke Tominaga

(Asian Spectroscopy Conference, 2020)

In this study we performed 2D-IR spectroscopic measurements on 9-fluorenone-4-carboxylic acid (FL-4) and 9-fluorenone-2-carboxylic acid (FL-2) in aqueous solutions. By comparing the results of FL-4 and FL-2, we aim to find the relationship between molecular structure and vibrational dynamics. The CO stretching bands of FL-4 and FL-2 are reproduced by a single Gaussian function and a sum of two Gaussian functions, respectively. Based on our previous work, we assigned the higher and lower bands in the IR spectrum of FL-2 to a complex of FL-2 and one D₂O and a complex of FL-2 and two D₂O, respectively. 2D-IR measurement provides information on the correlation of the vibrational spectrum at the pump

frequency (ω_1) and probe frequency (ω_3). The off-diagonal component at $(\omega_1, \omega_3) = (1694 \text{ cm}^{-1}, 1709 \text{ cm}^{-1})$ may have information about the chemical exchange process occurring between the two hydrogen-bonded complexes. Therefore, we analyzed the 2D-IR spectra to obtain dynamical information of the hydrogen-bond making and breaking processes between the CO group and surrounding water molecules. Moreover, to obtain microscopic details of the system, we also conducted molecular dynamics (MD) simulation. By analyzing the trajectories obtained by MD simulation, we found that hydration structure around the CO group of FL-2 is largely different from that of FL-4. Consequently, the hydrogen bond dynamics between the CO group and water molecules differ between FL-2 and FL-4.

II-B. DYNAMICS OF ELECTRONICALLY EXCITED STATE IN CONDENSED PHASES

Understanding of dynamics in the electronically excited state is a key issue to elucidate mechanisms in various photochemical reactions in condensed phases. It is also important for designing and developing new materials which have characteristic functions. We employ various kinds of ultrafast technique to monitor photochemical and photophysical events in sub-pico- to picoseconds time scales. By femtosecond fluorescence up-conversion technique, dynamics in the electronically excited state can be observed with a time resolution up to 100 fs. Vibrational dynamics in the electronically excited can be investigate by UV/VIS-pump IR probe technique. Moreover, low-frequency responses by photoexcitation are investigated by UV/VIS-pump THz probe experiment. Such responses include change of low-frequency vibrational modes induced by photoexcitation and photo-induced changes of charge carrier dynamics.

Dynamic Behavior of Photogenerated Charge Carriers in Diketopyrrolopyrrole-Linked Tetrabenzoporphyrin-Based Bulk Heterojunction Thin Films Probed with Time-Resolved Terahertz Spectroscopy

Kaoru Ohta, Yuichi Hiramatsu, Kohtaro Takahashi,¹ Mitsuharu Suzuki,¹ Hiroko Yamada,¹ and Keisuke Tominaga

¹Nara Institute of Science and Technology
(*J. Photochem. Photobiol.*, 2020)

Understanding of charge carrier dynamics on a picosecond time scale is very important for generation and relaxation of charge carriers in organic photovoltaic solar cells. Here, we study the dynamics of photogenerated charge carriers of diketopyrrolopyrrole-linked tetrabenzoporphyrin (C4-DPP-BP) bulk heterojunction (BHJ) thin films mixed with [6,6]-phenyl-C₆₁-butyric acid methyl ester

(PC₆₁BM) by subpicosecond time-resolved terahertz (THz) spectroscopy. It was found that the decay time constants of time-resolved THz signal in C4-BHJ films are 0.5 and 14 ps with a remaining offset at 800 nm-excitation when excitation fluence was 540 μJ/cm². The time-resolved THz signals result from bound polaron pairs where the charge carriers are dressed with phonons rather than from the excitons. These polaron pairs are generated by charge separation of the excitons. In contrast to neat films, the amplitudes of the subpicosecond-decaying components are sensitive to the fluence of the pump pulse. At higher fluence, these amplitudes increase due to the polaron pair annihilation process. At lower fluence, the transfer of the charge carriers from C4-DPP-BP to PC₆₁BM at the interface was clearly observed prior to the charge carrier quenching and generation of mobile charge carriers is enhanced compared to that of neat films.

Charge Transfer Dynamics of 9-Arylcarbazole Studied by Femtosecond Transient Absorption Spectroscopy

Kazuya Takamoto, Yoshifumi Ueno,¹ Kaoru Ohta, Seiji Akimoto,¹ Ryosuke Matsubara,¹ and Keisuke Tominaga

¹Graduation School of Science, Kobe University
(*Asian Spectroscopy Conference*, 2020)

Intramolecular charge transfer (ICT) in solutions is one of the most basic reactions, and the reaction mechanism of ICT is influenced by not only solute-solvent interactions but also geometrical change of solute molecule. 3,6-Bis(dimethylamino)-9-(4-cyanophenyl)carbazole (BANCC, Figure 1) consists of an electron donor of the carbazole unit and an acceptor of the cyanophenyl unit, which are connected by a single bond. In order to elucidate the ICT reaction mechanism of BANCC, we performed real time observation of the reaction process in various organic solvents by femtosecond transient absorption (TA) spectroscopy. We also performed measurements on 3,6-bis(dimethylamino)-carbazole (BAC), a molecule of the electron donor part of BANCC.

The absorption spectra of BANCC show two bands at 340 nm and 390 nm with no solvent dependence. These spectral features are the same as those of BAC. On the other hand, the fluorescence spectra of BANCC show a red shift as the solvent polarity increases, while those of BAC are less solvent-dependent. This result suggests that the excited state of BANCC is the ICT state with a large

dipole moment. In the observed TA spectra of BANCC in dimethylsulfoxide (DMSO) following excitation at 400 nm, a band emerges at 680 nm immediately after photoexcitation, and a new band rises at 550 nm together with decay of the band at 680 nm. Because the band at 680 nm is similar to the observed TA spectra of BAC, it is considered that the carbazole unit is locally excited by photoexcitation followed by charge transfer to the cyanophenyl group. Furthermore, a peak of the band at 550 nm shows a blue shift with a time constant of ~ 3 ps, which is similar to the solvation time of DMSO. The time constants of the blue shift in other solvents also show values close to the solvation times of these solvents. This suggests that the static and dynamic properties of the solvent have an effect on the ICT reaction.

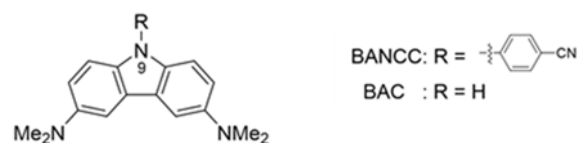


Figure 1. Molecular structures of BANCC and BAC.

I-C. MOLECULAR DYNAMICS IN THE TERAHERTZ FREQUENCY REGION IN CONDENSED PHASES

Vibrational spectroscopy has been widely used to investigate structures, interactions and dynamics of molecules and molecular complexes. The low-frequency region below several terahertz (THz; 1 THz = 33.3 cm^{-1}) corresponds to intermolecular modes of complexes and intramolecular modes with a weaker potential force and/or larger reduced mass. Intermolecular interactions such as hydrogen bonding, van der Waals forces and charge-transfer interactions play important roles in various chemical and biological processes. Moreover, the low-frequency spectra also reflect molecular dynamics on a time scale from picoseconds to femtoseconds.

There has been dramatic progress in the generation and detection techniques of freely propagating THz radiation in the past two decades. The examples of the generation technique include photoconductive switching, optical rectification, and the surface photocurrent of semiconductors. Because the pulse duration of the THz radiation is in a sub-picosecond time region, it is possible to measure the electric field of the radiation by

coherent detection methods, which consequently allows us to conduct THz time-domain spectroscopy (TDS). By THz-TDS the refractive index and extinction coefficient of a medium are obtained by measuring the phase and amplitude of the radiation. THz-TDS is an attractive method for studying dynamics in condensed phases with time scales of sub-picoseconds and picoseconds. We have applied THz-TDS to investigate the low-frequency dynamics of various kinds of condensed materials, including neat liquids and mixtures of liquids, biological polymers, and conducting polymers.

Interpretation of THz Intensities of Molecular Crystals: the Role of Mixing between Intermolecular and Intramolecular Vibrations

Feng Zhang, Hong-Wei Wang¹, Keisuke Tominaga, Michitoshi Hayashi¹, Masahiko Tani²

¹National Taiwan University

²University of Fukui

(IRMMW-THz, 2020)

Tani and coworkers reported the THz spectra of DL-alanine, L-alanine, and D-alanine in 2005. The racemic and enantiomeric compounds display completely distinct absorption features in the examined frequency range of 30-95 cm⁻¹. DL-alanine shows a major peak about 42 cm⁻¹, while D-alanine and L-alanine have two major peaks around 74 and 86 cm⁻¹, respectively. We calculated the THz modes for DL-alanine and L-alanine. All the observed THz peaks have been reproduced. Using previously developed

mode-analysis methods, we decomposed each of the three observed THz modes into a linear combination of intermolecular translation, intermolecular librations, and intramolecular vibration. In all the three modes, intermolecular translations make the dominant contributions to the vibrational energies (>96%), while the contributions from intramolecular vibrations are generally smaller than 2%. In order to evaluate the roles played by the intermolecular and intramolecular vibrations to the IR intensities, we calculated the contributions of each of the five forms of motions to the Born charge vectors. We found the non-ignorable roles played by the intramolecular vibrations in the determination of IR intensities in all the three modes. In particular, the intramolecular vibrations are the principal components of the Born charge vectors of mode for the DL-alanine and L-alanine cases.

Determination of the Fine Structure of a Halide Perovskite using High-resolution THz Spectroscopy and Solid-state Density Functional Theory

Feng Zhang, Izuru Karimata¹, Hong-Wei Wang², Takashi Tachikawa, Keisuke Tominaga, Michitoshi Hayashi², Tetsuo Sasaki³

¹Graduate School of Science, Kobe University

²National Taiwan University

³Shizuoka University

(IRMMW-THz, 2020)

Many types of disorders exist in the crystalline states and affect the physical and chemical properties of the crystals. The short-range correlations of disorder is one of the central issues of crystallography. In our previous studies we demonstrated a capability of THz spectroscopy to detect the fingerprint vibrational peaks of correlated molecular arrangements at the

nano-scale level in an occupation disorder system. THz spectroscopy may have, therefore, a promising potential to be a critical complementary tool to the X-ray and neutron diffraction methods in the structural analysis of disorder. In this work, we study the fine structure of the halide perovskite system ($\text{CH}_3\text{NH}_3\text{PbBr}_3$) where the short-range correlations of the disordered methylammonium (MA) cations remains an open question. Since each unit cell contains four MA molecules and each MA has two ways of orientations, there are in total 16 correlation possibilities of the MAs in one unit cell. We

considered the 16 correlations patterns and show the calculated normal modes. We also examined the correlation patterns of the MAs at a larger scale by constructing a supercell model. The model produces, however, additional THz peaks not observed in the experimental observation. We, therefore, conclude that the 16 correlation possibilities have been complete for representing the primary structures of his system. Based on the above conclusion, we suggest the halide perovskites contain ferroelectric regions within the nano-scale.

Broadband dielectric spectroscopy from sub-GHz to THz frequency region on hydrated bentonite

Lou Serafin M. Lozada, Alvin Karlo G. Tapia,¹ Armida V. Gillado,¹ Naoki Yamamoto,² and Keisuke Tominaga

¹University of the Philippines, Los Banos

²Jichi Medical University

(Asian Spectroscopy Conference, 2020)

Understanding how water molecules interact with one another and with clay under a confined geometry at different temperatures are key information in energy storage applications and nuclear waste disposal. Here we present an investigation of the dielectric response from 100 MHz to 1.8 THz of sodium bentonite at different hydration levels from 233 K to 293 K. Our previous studies have shown that for hydrated soft matters such as protein and lipid bilayers the dielectric response in the frequency region from sub-GHz to THz are due to the relaxation processes and vibrational processes, which are modeled using a Cole-Cole

function and Lorentzian function, respectively. The first term is the ion conductivity term, which may be important for conducting materials. We found that two Cole-Cole functions and one Lorentzian function are needed to reproduce both the imaginary and real parts of the complex dielectric spectra at room temperature. There is almost no intensity in the spectra for the dry bentonite ($h = 0$) from sub-GHz to sub-THz. However, both the real and imaginary parts of the complex dielectric spectra increased upon hydration. The fast relaxation time at 293 K is close to the bulk water Debye relaxation time of 9.5 ps. This suggests that there are freely moving bulk-like water molecules that may reside outside the interlayer. On the other hand, the major relaxation component has a time constant that is two orders of magnitude slower corresponding to interlayer water. It is suggested that most of the confined water in bentonite is highly restricted in its motion.

II-D. INTERMOLECULAR INTERACTIONS OF POLYMER STUDIED BY TERAHERTZ SPECTROSCOPY

Low-frequency vibrational bands observed in the low-frequency Raman and terahertz (THz) spectra originate from the higher-order structure, crystalline structure, and intermolecular interactions of polymer materials. Therefore, THz and low-frequency Raman spectroscopy are unique techniques for analyzing higher-order conformations and intermolecular hydrogen bonding in semi-crystalline polymers. However, the band assignment of THz spectra of polymers has not been studied well. Therefore, it is necessary to develop band assignment methods in order to establish THz spectroscopy as a powerful and unique method for exploring the structure and physical properties of polymers.

Differences in Intermolecular Interactions and Flexibility between Poly(ethylene terephthalate) and Poly(butylene terephthalate) Studied by Far-Infrared/Terahertz and Low-Frequency Raman Spectroscopy

Y. Yamamoto, H. Hoshina¹, H. Sato

¹Center for Advanced Photonics, RIKEN

(*Macromolecules*, 2021)

Herein, differences in the intermolecular interactions and flexibility between poly(ethylene terephthalate) (PET) and poly(butylene terephthalate) (PBT) are studied by far-infrared, terahertz (THz), and low-frequency Raman spectroscopy and quantum chemical calculations (QCCs). Interatomic distance calculations based on the reported crystal structures and natural bond orbital analysis indicate that PBT exhibits intermolecular hydrogen bonding between a C=O group and a CH₂ group in the adjacent molecular chains, while PET does not have such hydrogen bonding. The results of infrared measurements also suggest that the C=O and CH₂ groups of PBT are involved in intermolecular hydrogen bonding. Both PET and PBT show a THz band at around 113 cm⁻¹ and a Raman band at around 111 cm⁻¹. These bands indicate different thermal behaviors of PET and PBT. The results of QCCs performed using the Cartesian

coordinate tensor transfer method suggest that these bands of PBT include the CH₂ bending mode, while those of PET have only a small contribution from the corresponding mode. These differences in the thermal behavior and vibrational modes of the 113 cm⁻¹ bands can be possibly attributed to the difference in flexibility between PET and PBT due to the different number of CH₂ groups.

In addition, these bands of PBT seem to reflect the intermolecular C=O···H-C hydrogen bonding. Therefore, it may be concluded that the difference in the number of CH₂ groups causes the difference in the flexibility of the molecular chains between PBT and PET and the existence or non-existence of intermolecular C=O···H-C hydrogen bonding. It is worth noting that THz and low-frequency Raman spectroscopy can clearly reveal the difference in flexibility. It is also very likely that both the flexibility of the molecular chains and the intermolecular hydrogen bonding affect the difference in the crystallization rate between PET and PBT.

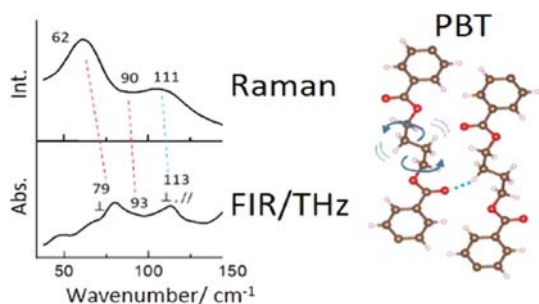


Figure 1. FIR/THz and low-frequency Raman spectra of PBT.

Study of changes in water structure and interactions among water, CH₂, and COO⁻ groups during water absorption in acrylic acid-based super absorbent polymers using Raman spectroscopy

T. Nasu, H. Sato

(Spectrochimica Acta Part A, 2020)

The interactions of acrylic acid-based super absorbent polymers (SAPs) with water and the hydrogen bonding of water within its three-dimensional network were studied using Raman spectroscopy. The Raman spectra of SAP solutions suggested that both the COO⁻ and CH₂ groups of SAPs interact with water. The Raman spectra of pure water and those of SAPs containing approximately 40, 50, and 60% water exhibited a broad band corresponding to the OH-stretching mode of water in the 4000 – 3000 cm⁻¹ region. This band was separated into three components using a curve-fitting method. The three components at 3200, 3400, and 3600 cm⁻¹ were assigned to the OH-stretching modes of strong hydrogen bonding (SHB), weak hydrogen bonding (WHB), and dangling bond (Dang) species of water, respectively. The fractional areas of the three components were calculated and compared. The changes in the hydrogen bonding of water were compared with those of the water present

in SAPs, and their temperature-dependent variations were elucidated. At a water content of approximately 60%, the behavior of the fractional area versus temperature was similar to that of pure water. However, at a water content of approximately 40%, the behavior was significantly different. The fraction of SHB was smaller, and the fraction of WHB was larger than that of pure water. The difference in the CH and COO⁻ peak shifts of SAP, which is a result of the addition of a small percentage of water, was revealed by Raman spectroscopy. The position of the CH₂ deformation peak changed linearly. However, the position of the COO⁻ rocking peak did not change significantly up to a water content of 30%, above which it exhibited a rapid shift to lower wavenumbers. This result indicates that the interactions of the CH₂ and COO⁻ groups are different.

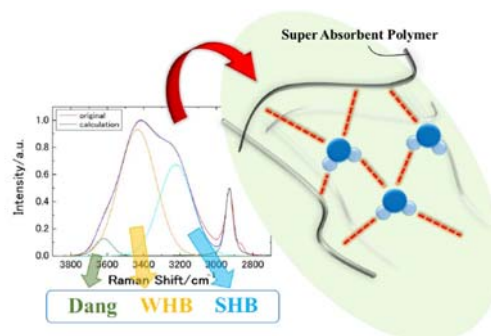


Figure 1. Three kinds of OH stretching modes of water; SHB, WHB, and Dang in the super absorbent polymer.

Intermolecular hydrogen bonding of polymer by terahertz and low-frequency Raman spectroscopy

H. Sato

(The 10th International Symposium on Two-dimensional Correlation Spectroscopy (IW-FIRST 2021))

The weak C-H···O hydrogen bonds of polymers play a crucial role in stabilizing the crystalline lamellae and folding of the molecular chain of polymers, and it has a significant effect on the physical properties of the polymer. Terahertz (THz) and low-frequency Raman spectroscopy can provide information on the higher-order structure and intermolecular hydrogen bonding of polymers. Therefore, by performing FIR, THz or low-frequency Raman spectra measurements with quantum chemical calculations (QCCs), we have investigated the weak hydrogen bonding in the crystalline structure of polyesters.

THz and low-frequency Raman spectroscopy successfully detected the different types of intermolecular hydrogen bonds in the lamellar structure of polycaprolactone (PCL), a changing in the inter- and intramolecular hydrogen bonds of polybutylene succinate (PBS) by stress-induced crystal transition, and the differences in the mobility

of molecular chains and intermolecular hydrogen bondings between poly(ethylene terephthalate) (PET) and poly(butylene terephthalate) (PBT), and so on. Furthermore, THz imaging was successfully used to visualize the distribution of crystallinity and crystal orientation in polymer films. In the future, it is expected that THz and low-frequency Raman spectroscopy will be more widely used to evaluate the physical properties of polymer materials.

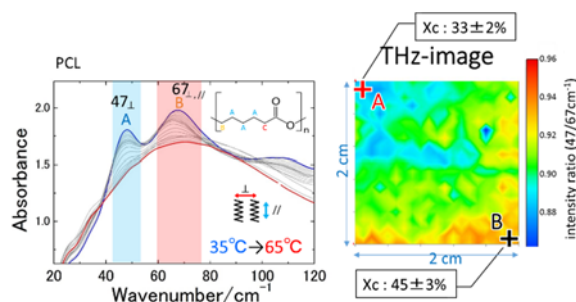


Figure 1. Temperature-dependent THz spectra of PCL in the temperature range of 35 to 65 °C, and a THz imaging of distribution of crystallinity of PCL film.^[1]

[1] C. Funaki, S. Yamamoto, H. Hoshina, Y. Ozaki, and H. Sato, *Polymer*, **137** (2018) 245.

[2] C. Funaki, T. Toyouchi, H. Hoshina, Y. Ozaki, and H. Sato, *Applied Spectroscopy*, **71** (2017) 1537.

[3] Y. Yamamoto, H. Hoshina, and H. Sato, *Macromolecules*, in press (2021).

III Terahertz Material Physics Laboratory

III-A. HIGH FIELD ELECTRON SPIN RESONANCE (ESR) STUDIES OF QUANTUM SPIN SYSTEMS

The quantum effects and the spin frustration effects prevent long-range order due to strong quantum fluctuation and frustration. Their ground states at low temperature are attractive issue in field of solid state physics. High-frequency high-field ESR is a powerful spectroscopic method to investigate the ground state and lower excited state of the system, because the ESR observes directly the magnetic excitation. Following the trends from a Grant-in-Aid for Scientific Research on Priority Areas “Novel states of matter induced by frustration” (No.473, 2007-2011, Headed by Prof. H. Kawamura (Osaka University) and H. Ohta was a member), we are studying these low dimensional antiferromagnets with frustration and related multiferroic materials intensively. Appearance of breather, soliton and antisoliton modes are expected in wide frequency-field ESR measurements of $S = 1/2$ Heisenberg antiferromagnetic chain with staggered D vector system $\text{KCuMoO}_4(\text{OH})$. We succeeded in observing these signals using micro-single-crystal of $\text{KCuMoO}_4(\text{OH})$. The magnetic anisotropy of breather excitations, soliton and antisoliton modes have been revealed. Following researches have been also performed by the joint research program of Molecular Photoscience Research Center, Kobe University. We continued collaborations with H. Kikuchi's group in University of Fukui for quantum spin systems. Exotic Co system CoSeO_3 has fruitful magnetic phases. High field ESR and magnetic torque measurements of CoSeO_3 revealed anomalous spin reorientations under magnetic fields. For other joint researches, high-field ESR and the magnetic susceptibility measurements of thin film of neodymium permanent magnets have been performed to obtain information of the magnetic anisotropy. And we also have joint research with theoretical groups for obtaining experimental parameter from quantum calculations. In total, our joint researches have been performed with 19 groups, and we have organized one scientific meeting with joint research groups.

H. Ohta is continuing as the Immediate-Past President of IES (2018-2020) after finishing the President (2015-2017) of the International EPR (ESR) Society (IES). H. Ohta is also acting as the Advisory Council of APES (Asia-Pacific EPR/ESR Society), and the Council Member of the Society of Electron Spin Science and Technology (SEST). H. Ohta is the Local Organizing Committee Chair and S. Okubo is the member of the fund-raising committee of the ISMAR-APNMR2021 which will be held in Aug., 2021 as the on-line conference.

Moreover, in order to strengthen the pulsed magnetic field researches in the western Japan region, we have been continuing the activities of The KOFUC (Kobe-Osaka-Osaka Prefecture-Fukui Universities Centers) Network since 2014.

Development of Eu²⁺ and Mn²⁺ co-activated silicate phosphor for plant cultivation light source

Takashi Kunimoto¹, Yoshiko Fujita¹, Hiroshi Kajiyama¹, Tetsuo Honma², Hideki Kawaguchi³, Tadashi Ishigaki³, Koutoku Ohmi³, Kentaro Ohshima⁴, Daisuke Miyazaki⁴, Yu Saito⁵, Shigeo Hara⁵, Takahiro Sakurai⁵, Susumu Okubo⁶, and Hitoshi Ohta^{4,6}

¹Department of Nano Material and Bio Engineering, Tokushima Bunri University

²Japan Synchrotron Radiation Research Institute

³Graduate School of Engineering, Tottori University

⁴Graduate School of Science, Kobe University

⁵Research Facility Center for Science and Technology, Kobe University

⁶Molecular Photoscience Research Center, Kobe University

(*Jpn. J. Appl. Phys.*, 2019)

Various light sources for plant production have been developed to establish a completely controlled factory.

We propose a pulse light source using Xe discharge. For the rapid growth of the plant, an intense light covering the absorption spectral region of chlorophyll is demanded, and periodic irradiation is also required because the photosynthetic reaction has a certain period. In this study, Sr₃MgSi₂O₈:Eu, Mn phosphor powders with various Eu and Mn content, which show two emission peaks in the absorption region of photosynthetic pigment and phytochrome, were synthesized, and were analyzed using X-ray diffraction, photoluminescence and electron spin resonance spectroscopy. It was found that the exchange-coupled Mn-Mn and Eu-Mn pairs lead the rapid decay of Mn emission and efficient energy transfer from Eu and Mn ions, respectively. A plasma tube array panel using the phosphor was also fabricated and the similar emission spectrum of Sr₃MgSi₂O₈:Eu,Mn is obtained under vacuum-UV excitation in comparison to the UV excitation.

II-B. DEVELOPMENT OF NOVEL ESR TECHNIQUES IN THE THz REGION USING MICROMECHANICAL DEVICES

Force detection of ESR signal is a powerful tool in sensitive detection of small-volume samples. In this technique, sample magnetization changes accompanied by ESR absorption are converted to a field-gradient force exerted on a SiNx nanomembrane. The force-detected ESR technique using a 10 T split-pair superconducting magnet was newly developed. We applied this technique to non-centrosymmetric magnet CuB₂O₄, and revealed from the angle-dependent ESR measurement that the ESR signals observed in the ordered phase are attributable to paramagnetic resonance, rather than antiferromagnetic resonance.

Another promising application of force-detected ESR is metalloprotein. However, the low spin concentration generally makes ESR detection of these samples quite difficult. To solve this problem, we combined our technique with high-power terahertz source, gyrotron, installed at Fukui University, and successfully improved the detection sensitivity. Measurements were carried out at Fukui University with helps of Dr. Ishikawa and Prof. Mitsudo. ESR signals of DPPH and CuPzN were observed at room temperature. In the future, this technique will be applied to hemoproteins.

We also developed a novel high-frequency ESR technique exploiting thermal process accompanied with ESR absorption. With a sample attached at the end of cantilever beam, temperature at the beam end increases due to thermal relaxation when the ESR condition is met. The resultant temperature gradient is sensitively measured using a thermocouple. The advantages are high sensitivity, small background, and wide temperature range. We succeeded in multi-frequency ESR measurement of DPPH at various temperatures. Practical applications to various magnetic samples will be promising in the near future.

Collaborative research with Dr. Horitani at Saga University was also carried out. ESR signals of model compounds were observed, but further sensitivity improvement is needed for more detailed analysis. H. Takahashi also conducted the research project from JST-PRESTO's program "Thermal Science and Control of Spectral Energy Transport", in which the heat transport of magnetic materials was studied by high-frequency ESR spectroscopy.

Prof. Ohta gave invited talks regarding nanomembrane-based ESR in the terahertz region at "Modern Development of Magnetic Resonance" and "International Conference on Infrared, Millimeter, and Terahertz Waves (IRMMW-THz 2020)". H. Takahashi gave an invited talk at "The 8th International Workshop on Far-Infrared Technologies (IW-FIRT 2021)".

Zero - Field Splitting Parameters of Hemin Investigated by High - Frequency and High - Pressure Electron Paramagnetic Resonance Spectroscopy

E. Ohmichi¹, T. Okamoto¹, T. Sakurai², H. Takahashi³, S. Okubo³, H. Ohta³

¹Graduate School of Science, Kobe University

²Research Facility Center for Science and Technology, Kobe University

³Molecular Photoscience Research Center, Kobe University

(Appl. Mag. Res., 2020)

We systematically studied the zero-field splitting (ZFS) parameters of Fe(III) protoporphyrin IX chloride, or hemin, using the terahertz electron paramagnetic resonance (EPR) spectroscopy technique at ambient and high pressures. Although

hemin is known as a model substance of hemoproteins, the pressure effect on the electronic structure has not yet been explored owing to the large ZFS. In this study, high-field and high-frequency EPR measurements were carried out in the frequency range up to 700 GHz and at hydrostatic pressures up to 2 GPa. At ambient pressure, multiple EPR branches were clearly observed, and the axial and rhombic components of ZFS were determined as $D = 6.90 \pm 0.01 \text{ cm}^{-1}$ and $E = 0.055 \pm 0.005 \text{ cm}^{-1}$, respectively. Upon pressure application, we observed a systematic shift of the resonance field, indicating a monotonous increase of the axial component from $D = 6.9$ to 7.9 cm^{-1} at 2 GPa. The origin of this unusually large shift was discussed from a microscopic viewpoint of the electronic structure of iron under pressure.

Mechanically Detected Terahertz Electron Spin Resonance

E. Ohmichi¹, T. Okamoto¹, H. Takahashi², H. Ohta²

¹Graduate School of Science, Kobe University

²Molecular Photoscience Research Center, Kobe University

(*Appl. Mag. Res.*, 2021)

In this review, mechanically detected electron spin resonance (MDESER) in the terahertz (THz) region is

described to demonstrate its usability as a novel methodology for obtaining microscopic insights into local electronic structures. Using micromechanical devices, the sensitivity to a small-volume sample is greatly enhanced even for a cavityless setup. Moreover, there are plenty of options in the setup of MDESER, including detection modes, mechanical devices, and detection techniques. ESR spectroscopy of single-crystalline, powder, and frozen solution samples in the THz region are demonstrated.

Force detection of high-frequency electron spin resonance near room temperature using high-power millimeter-wave source gyrotron

H. Takahashi¹, Y. Ishikawa², T. Okamoto³, D. Hachiya³, K. Dono², K. Hayashi², T. Asano⁴, S. Mitsudo², E. Ohmichi³, and H. Ohta¹

¹Molecular Photoscience Research Center, Kobe University

²Research Center for Development of Far-Infrared Region, University of Fukui

³Graduate School of Science, Kobe University

⁴Department of Applied Physics, University of Fukui
(*Appl. Phys. Lett.*, 2021)

We report the measurement of force-detected electron spin resonance (FDESER) at 154 GHz using a gyrotron. The high output power allows the use of a strong transverse magnetic field larger than 10^{-4} T, which is sufficient to cause ESR saturation. We obtained the FDESER signal with a high spin sensitivity on the order of 10^{12} spins/G at 280 K. Our system has promising applications in high-frequency ESR studies of low-spin concentration samples, such as metalloprotein solutions.

This study was partially supported by the Murata Science Foundation.

III-C. DEVELOPMENT AND APPLICATION OF HIGH-PRESSURE THz ESR SYSTEM

High pressure THz ESR is a very powerful means to clarify the pressure effect of magnetic materials. One of the features of our high pressure ESR system is the use of a piston-cylinder pressure cell which has both good transmittance of electromagnetic wave in THz region and a maximum pressure of 2.5 GPa. However, there remained a problem in accurate pressure calibration for this system. Therefore, we have developed a new system with induction coils outside the pressure cell, which enable AC magnetization measurement of tin set inside the pressure cell. The superconducting transition temperature of tin depends the pressure and the relationship can be used for pressure calibration. This system enables accurate pressure calibration in addition to the conventional transmission-type ESR measurement for a sample set in the pressure cell. Furthermore, we manufactured a new cylinder with a slightly smaller inner diameter than the previous one

and succeeded in expanding the pressure range to 2.8 GPa. Using this system, a typical paramagnet cobalt Tutton's salt was measured, and the g principal values were determined at 0 GPa for the first time. Owing to the high spectral resolution of this system, the in-plane anisotropy was observed in the cobalt Tutton's salt, which was believed to have uniaxial anisotropy. Moreover, it was found that the g principal values change significantly with pressure. A master course student M. Yasutani received the poster award at the 29th Japan Society of Infrared Science and Technology annual meeting (29-30 October, online) on his development of this high-pressure ESR system and its application.

In addition, the thermal detection type ESR was applied to the high pressure ESR measurement. A thermocouple was introduced into the pressure cell, and the ESR signal of the cobalt Tutton's salt was successfully detected as the temperature increase during resonance. We also succeeded in combining the developed probe with the split-pair magnets and obtaining the angle dependence of ESR signal of the cobalt Tutton's salt.

H. Ohta gave invited talks at Modern Development of Magnetic Resonance, and International Conference on Infrared, Millimeter, and Terahertz Waves (IRMMW-THz 2020) on the development of high-pressure THz ESR system and its application. T. Sakurai gave an invited talk at "International Workshop on Quantum Magnets in Extreme Conditions" especially on the application to the orthogonal dimer-spin system $\text{SrCu}_2(\text{BO}_3)_2$ (2021.3.22-26, online).

Pressure control of the magnetic anisotropy of the quasi-two-dimensional van der Waals ferromagnet $\text{Cr}_2\text{Ge}_2\text{Te}_6$

T. Sakurai¹, B. Rubrecht^{2,3}, L. T. Corredor², R. Takehara⁴, M. Yasutani⁴, J. Zeisner^{2,3}, A. Alfonso², S. Selzer^{2,3}, S. Aswartham², A. U. B. Wolter², B. Büchner^{2,5}, H. Ohta⁶, and V. Kataev²

¹Research Facility Center for Science and Technology, Kobe University

²Leibniz IFW Dresden

³Institute for Solid State and Materials Physics, TU Dresden

⁴Graduate School of Science, Kobe University

⁵Institute for Solid State and Materials Physics and Würzburg-Dresden Cluster of Excellence ct.qmat, TU Dresden

⁶Molecular Photoscience Research Center, Kobe University

(*Phys. Rev. B*, 2021)

We report the results of the pressure-dependent measurements of the static magnetization and of the ferromagnetic resonance (FMR) of $\text{Cr}_2\text{Ge}_2\text{Te}_6$ to address the properties of the ferromagnetic phase of this quasi-two-dimensional van der Waals magnet. The static magnetic data at hydrostatic pressures up to 3.4 GPa reveal a gradual suppression of ferromagnetism in terms of a reduction of the critical transition temperature, a broadening of the transition width, and an increase of the field necessary to fully saturate the magnetization M_s . The value of $M_s \approx 3\mu\text{B}/\text{Cr}$ remains constant within the error bars up to a pressure of 2.8 GPa. The anisotropy of the FMR signal continuously diminishes in the studied hydrostatic pressure range up to 2.39 GPa, suggesting a reduction of the easy-axis-type magnetocrystalline anisotropy energy (MAE). A quantitative analysis of the FMR

data gives evidence that up to this pressure the MAE constant KU , although getting significantly smaller, still remains finite and positive, i.e., of the easy-axis type. Therefore, a recently discussed possibility of switching the sign of the magnetocrystalline anisotropy in $\text{Cr}_2\text{Ge}_2\text{Te}_6$ could only be expected at still

higher pressures, if possible at all, due to the observed weakening of the ferromagnetism under pressure. This circumstance may be of relevance for the design of strain-engineered functional heterostructures containing layers of $\text{Cr}_2\text{Ge}_2\text{Te}_6$.

III-D. MAGNETIZATION MEASUREMENTS USING SQUID MAGNETOMETER

The installation of SQUID magnetometer in 2010 by a Grant-in-Aid Creative Scientific Research “Development of properties and functionalities by precise control of rare-earth doping” (2007-2011, Prof. Y. Fujiwara (Osaka University)) opened up wide varieties of collaborative researches. From 2010 applications of SQUID magnetometer to various material researches spread out continuously. It is also supporting the user programs of Molecular Photoscience Research Center, Kobe University since 2017. Users of SQUID magnetometer are Mochida and Takahashi group, Uchino group (Department of Chemistry, Kobe University), Sugawara and Matsuoka group, and Kotegawa and Tou group (Department of Physics, Kobe University), T. Sakurai, S. Hara and Y. Saito (Center for Supports to Research and Education Activities, Kobe University).

Magnetic and Transport Properties of New Cubic compounds $\text{Ce}_6\text{Pd}_{13}\text{Cd}_4$ and $\text{R}_6\text{Pd}_{13}\text{Zn}_4$ ($\text{R} = \text{Pr}$, Nd) with the Octahedral Rare-Earth Sublattices
Eiichi Matsuoka¹, Yasuo Iwakiri¹, Akihiro Oshima¹, Hitoshi Sugawara¹, Takahiro Sakurai², and Hitoshi Ohta³

¹Department of Physics, Graduate School of Science, Kobe University

²Research Facility Center for Science and Technology, Kobe University

³Molecular Photoscience Research Center, Kobe University
(JPS Conf. Proc., 2019)

Magnetic and transport properties of the cubic compounds $\text{Ce}_6\text{Pd}_{13}\text{Cd}_4$, $\text{Pr}_6\text{Pd}_{13}\text{Zn}_4$, and $\text{Nd}_6\text{Pd}_{13}\text{Zn}_4$ have been investigated by the magnetization, the electrical resistivity, and the specific-heat measurements. $\text{Ce}_6\text{Pd}_{13}\text{Cd}_4$ is an antiferromagnetic

Kondo-lattice compound with the transition temperature at $T_N = 2.9$ K. The increase in the magnetic susceptibility below T_N and the large value of the specific heat divided by temperature (1.47 J/Ce-mol K^2) imply the existence of non-ordered Ce magnetic moment due to the geometrical frustration on the octahedral Ce sublattice. No magnetic transition has been detected for $\text{Pr}_6\text{Pd}_{13}\text{Zn}_4$ above 0.62 K, while phase transition which is presumably due to antiferromagnetic order has been observed for $\text{Nd}_6\text{Pd}_{13}\text{Zn}_4$ at $T_t = 1.2$ K. The large values of the paramagnetic Curie temperature divided by transition temperature (>13.2 for $\text{Pr}_6\text{Pd}_{13}\text{Zn}_4$ and 5.1 for $\text{Nd}_6\text{Pd}_{13}\text{Zn}_4$) suggest that the magnetic transition temperatures are strongly suppressed by the geometrical frustration on the octahedral rare-earths sublattice.

Magnetic, Transport, and Thermal Properties of New Cubic Compounds $Ce_6Mg_{23}Z$ ($Z = C, Si, Ge$)

Ryota Shibuya¹, Eiichi Matsuoka¹, Hitoshi Sugawara¹, Takahiro Sakurai², and Hitoshi Ohta³

¹Department of physics, Graduate School of Science, Kobe University

²Research Facility Center for Science and Technology, Kobe University

³Molecular Photoscience Research Center, Kobe University

(*JPS Conf. Proc.*, 2019)

We have focused on new cubic compounds $Ce_6Mg_{23}Z$ ($Z = C, Si, Ge$) in which Ce atoms are reported to form

an octahedral sublattice. In this study, we have grown polycrystalline samples of $Ce_6Mg_{23}Z$ and studied their magnetic and transport properties. We found that the Ce ions in these compounds are trivalent and antiferromagnetic transition occurs at 1.6 and 1.2 K for $Ce_6Mg_{23}Ge$ and $Ce_6Mg_{23}Si$, respectively. The large values of the paramagnetic Curie temperature divided by the antiferromagnetic transition temperature (4.5 for $Ce_6Mg_{23}Ge$ and 9.9 for $Ce_6Mg_{23}Si$) imply suppression of transition temperature due to geometrical frustration on the octahedral Ce sublattice.

Proximity coupling of superconducting nanograins with fractal distributions

Takashi Uchino¹, Nanami Teramachi¹, Ryosuke Matsuzaki¹, Emi Tsushima¹, Shusuke Fujii¹, Yusuke Seto², Kazuyuki Takahashi¹, Takao Mori³, Yutaka Adachi⁴, Yukihito Nagashima⁵, Yoshifumi Sakaguchi⁶, Kazuki Ohishi⁶, Akihiro Koda⁷, Takahiro Sakurai⁸ and Hitoshi Ohta⁹

¹Department of Chemistry, Graduate School of Science, Kobe University

²Department of Planetology, Graduate School of Science, Kobe University

³International Center for Materials Nanoarchitectonics, National Institute for Materials Science

⁴Optoelectronic Materials Group, Optical and Electronic Materials Unit, National Institute for Materials Science

⁵Nippon Sheet Glass Co., LTD

⁶Neutron Science and Technology Center, Comprehensive Research Organization for Science and Society (CROSS)

⁷Institute of Materials Structure Science, High Energy Accelerator Research Organization

⁸Center for Support to Research and Education Activities, Kobe University

⁹Molecular Photoscience Research Center, Kobe University

(*Phys. Rev. B*, 2020)

We explore the electrical and magnetic properties of a fractal assembly of Josephson junctions with transparent interfaces. For this purpose, we employ an Mg/MgO/MgB₂ nanocomposite with ~16 vol. % of MgB₂ nanograins, which are distributed in a fractal manner in the normal matrix. Irrespective of the low volume fraction of MgB₂ nanograins, the nanocomposite behaves as a bulk-like superconductor, i.e., zero resistivity, perfect diamagnetism, and strong vortex pinning. Thus, a global Josephson phase coherence is achieved in the nanocomposite. The lower (H_{c1J}) and higher (H_{c2J}) critical fields of the Josephson network are exceptionally high ($H_{c1J} = 96$ Oe and $H_{c2J} = 83.5$ kOe) as compared to those reported

previously for granular superconductors. This will give an example of robust macroscopic superconducting coherence derived from long-range proximity coupling among fractally distributed superconducting nanograins through quantum interference of Andreev quasiparticles. Transverse-field muon spin rotation measurements reveal that the mean internal field in the superconducting mixed state

increases with decreasing temperature below which the Josephson phase coherence sets in, opposite to the diamagnetic response observed in magnetization measurements. This unusual behavior implies a highly disordered and fluctuating nature of the Josephson vortices in the present superconducting nanocomposite.

The Impact of the Next-Nearest Neighbor Dispersion Interactions on Spin Crossover Transition Enthalpy Evidenced by Experimental and Computational Analyses of Neutral π -Extended Heteroleptic Fe(III) Complexes

A. Miyawaki¹, T. Mochida^{1,2}, T. Sakurai³, H. Ohta⁴, and K. Takahashi¹

¹Department of Chemistry, Graduate School of Science, Kobe University

²Center for Membrane and Film Technology, Kobe University

³Research Facility Center for Science and Technology, Kobe University

⁴Molecular Photoscience Research Center, Kobe University

⁵Muroran Institute of Technology

⁶Department of Physics, Okayama University
(*Inorganic Chemistry*, 2020)

A neutral heteroleptic Fe(III) complex **1** derived from a π -extension of the parent complex **2** was prepared and characterized. Complex **1** exhibited an abrupt spin crossover (SCO) transition exactly at room temperature (TSCO = 298 K). A crystal structure

analysis of **1** revealed that the Fe(III) complex molecules formed a three-dimensional π -stacking interaction network. To thermodynamically clarify the mechanism of the SCO transition, the thermodynamic parameters of the SCO transitions for **1** and **2** were deduced from the temperature dependence of the magnetic susceptibility in the solid and solution states using the regular solution model. A comparison of the SCO enthalpy difference between the solid and molecule for **1** and **2** revealed that the lattice enthalpy difference would largely contribute to the SCO transition enthalpy difference. A computational evaluation of intermolecular interactions and lattice energies before and after the SCO transitions in **1** and **2** disclosed the significant contribution of the next-nearest neighbor dispersion interactions to the lattice enthalpy differences. This finding indicates that not only conventional nearest neighbor intermolecular interactions but also next-nearest neighbor dispersion interactions should be taken into account to understand the fundamental mechanism of a phase transition in molecular solids.

Synthesis, Structure, and Magnetic Properties of Linear Trinuclear CuII and NiII complexes of

Porphyrin Analogues Embedded with Binaphthol Units

**J. Setsune¹, S. Omae¹, Y. Tsujimura¹, T. Mochida¹,
T. Sakurai² and H. Ohta³**

¹Department of Chemistry, Graduate School of Science, Kobe University

²Research Facility Center for Science and Technology, Kobe University

³Molecular Photoscience Research Center, Kobe University

(*Symmetry*, 2020)

A porphyrin analogue embedded with (S)-1,1'-X-bi-2-naphthol units was synthesized without reducing optical purity of the original binaphthol unit. This new macrocyclic ligand provides the hexaanionic N₄O₄ coordination environment that enables a linear array of three metal ions. That is, it provides the square planar O₄ donor set for the central metal site and the distorted square planar N₂O₂ donor set for the terminal metal

sites. In fact, a Cu^{II}₃ complex with a Cu(1)–Cu(2) distance of 2.910 Å, a Cu(1)–Cu(2)–Cu(1') angle of 174.7°, and a very planar Cu₂O₂ diamond core was obtained. The variable-temperature ¹H-NMR study of the Cu^{II}₃ complex showed increasing paramagnetic shifts for the naphthyl protons as temperature increased, which suggests strong antiferromagnetic coupling of Cu^{II} ions. The temperature dependence of the magnetic susceptibility indicated antiferromagnetic coupling both for the Cu^{II}₃ complex ($J = -434 \text{ cm}^{-1}$) and for the Ni^{II}₃ complex ($J = -49 \text{ cm}^{-1}$). The linear (L)M(μ-OR)₂M(μ-OR)₂M(L) core in a rigid macrocycle cavity made of aromatic components provides robust metal complexes that undergo reversible ligation at the apical sites of the central metal.

Nonmagnetic first-order phase transition in the nonsymmorphic NbCrP

**Yoshiki Kuwata^{1,2}, Hisashi Kotegawa¹, Hideki Tou¹,
Hisatomo Harima¹, Qing-Ping Ding², Keiki Takeda³,
Junichi Hayashi³, Eiichi Matsuoka¹, Hitoshi Sugawara¹,
Takahiro Sakurai⁴, Hitoshi Ohta^{1,5}, and Yuji Furukawa²**

¹Department of Physics, Kobe University

²Ames laboratory, U.S. DOE and Department of Physics and Astronomy, Iowa State University

³Muroran Institute of Technology

⁴Research Facility Center for Science and Technology, Kobe University

⁵Molecular Photoscience Research Center, Kobe University

(*Phys. Rev. B*, 2020)

We report the discovery of a first-order phase transition at around 125 K in NbCrP, which is the nonsymmorphic crystal with Pnma space group. From the resistivity, magnetic susceptibility, and nuclear magnetic resonance measurements using crystals made by the Sn-flux method, the high-temperature (HT) phase is characterized to be metallic with a non-negligible magnetic anisotropy. The low-temperature (LT) phase is also found to be a nonmagnetic metallic state with a crystal of lower symmetry. In the LT phase, the spin susceptibility is reduced by ~30% from that in the HT phase, suggesting that the phase transition is triggered by the electronic instability. The possible origin of the phase transition in NbCrP is discussed based on the electronic structure by comparing it with those in other nonsymmorphic compounds RuP and RuAs.

III-E. DEVELOPMENT OF NEW MICROWAVE SPECTROSCOPY TECHNIQUES

The dynamics of superconducting vortices in unconventional superconductors is expected to have different characteristics from those in conventional superconductors. In particular, the Hall effect caused by flux flow is interesting because it provides us insights into the quasiparticle states inside the vortex core. However, its observation requires electromagnetic waves with frequencies higher than microwaves to eliminate the effect of vortex pinning. Takahashi developed a microwave Hall effect measurement method using a cross-shaped bimodal microwave resonator with Professor Maeda's group at the University of Tokyo.

Microwave Hall effect measurement for materials in the skin depth region

Ryo Ogawa¹, Tatsunori Okada², Hideyuki Takahashi³, Fuyuki Nabeshima¹ and Atsutaka Maeda¹

¹Department of Basic Science, The University of Tokyo

²Institute for Materials Research, Tohoku University,

³Molecular Photoscience Research Center, Kobe University

(J. Appl. Phys., 2021)

We developed a new microwave Hall effect measurement method for materials in the skin depth region at low temperatures using a cross-shaped bimodal cavity. We analytically calculated electromagnetic fields in the cross-shaped cavity and the response of the cavity including the sample, whose

property is represented by the surface impedance tensor; furthermore, we constructed the method to obtain the Hall component of the surface impedance tensor in terms of the change in resonance characteristics. To confirm the validity of the new method, we applied our method to measure the Hall effect in metallic Bi single crystals at low temperatures, and we confirmed that the microwave Hall angles coincide with the DC Hall angle. Thus, it becomes clear that the Hall angle measurement under cryogenic conditions becomes possible without any complicated tuning mechanisms, and our bimodal cavity method can be used to measure the microwave Hall effect on materials in the skin depth region. The result opens a new approach to discuss the Hall effect in condensed matter physics such as the microwave flux-flow Hall effect in superconductors.

III-F. SPIN AND LATTICE DYNAMICS STUDIED BY PUMP-PROBE AND TERAHERTZ SPECTROSCOPIES

The terahertz region in the electromagnetic spectrum has attracted research attention in solid-state physics, because elementary excitations in solid-state materials such as phonons and magnons play important roles, and many of those dynamics appear in this energy region. The ultrafast spin dynamics and optical spin control in magnetic materials are attractive topics because of the potential applications in the developments of ultrafast spin control, spintronics, quantum computing, and optical control of correlated spin systems. We studied the spin and lattice dynamics in solid-state materials using optical pump-probe spectroscopy and terahertz time-

domain spectroscopy (THz-TDS). The generation and detection of magnetization and birefringence using optical and electric pulses are very useful to observe the spin and lattice dynamics in ferromagnetic, antiferromagnetic, multiferroic, and magnetoelectric materials. The time-domain spectroscopy has a large potential for the ultrafast, broadband, and accurate observation of elementary excitation dynamics in the terahertz region.

Terahertz time-domain spectroscopy in antiferromagnetic cobalt oxide

Y. Iwasaki¹, M. Kita¹, Y. Kokogawa¹, T. Moriyasu², and T. Kohmoto^{1,3}

¹Graduate School of Science, Kobe University

²University of Fukui

³Molecular Photoscience Research Center, Kobe University

(iCAMP 2020)

The absorption of the 4.4-THz magnon mode in cobalt oxide (CoO), which is antiferromagnetic below the Néel temperature ($T_N = 290$ K), was observed by terahertz time-domain spectroscopy (THz-TDS) using air plasma.

Magnons are magnetic elementary excitations in magnetic materials, which are quantized spin waves. At room temperature, CoO has a rock-salt type cubic crystal structure and is paramagnetic, while, below T_N , it has a tetragonal crystal structure and is antiferromagnetic (AFM). In the AFM phase, cobalt spins align ferromagnetically within a (111) plane, and these planes are stacked antiferromagnetically in the direction normal to (111) planes. In the present study, we attempted to observe magnon absorption of CoO in

the time domain by THz-TDS using broadband THz waves. In the experiment, CoO samples with (100) plane orientation and the thickness of 0.1, 0.5, 0.9, and 3.0 mm were used.

From the Fourier spectra of the transmitted THz electric field observed at 5 K, it is confirmed that the 0.9-mm CoO has a slight dip near 4.5 THz. It is found that the spectral amplitude above 4 THz is considerably reduced in the 3.0-mm CoO. It is considered that this is because the absorption in the higher frequency region increases as the thickness increases, due to the influence of the phonon-absorption tail of CoO that has a peak on the higher frequency side.

From the temperature dependence of the normalized transmission spectrum of the THz electric field observed in the 0.9-mm CoO, it is confirmed that there is a dip near 4.4 THz at 5 K and 50 K, but the dip disappears at the temperature of 100 K or higher. It is thought that this is because the influence of the tail of the phonon absorption increases as the temperature increases, the spectral amplitude of the high-frequency components decreases, and the absorption of magnon becomes invisible.

Lattice dynamics in an antiferromagnet chromium oxide

Y. Maeda¹, S. Kawabata¹, H. Taniguchi¹, R. Hikita¹, and T. Kohmoto^{1,2}

¹Graduate School of Science, Kobe University

²Molecular Photoscience Research Center, Kobe University

(iCAMP 2020)

In recent years, various types of multiferroic materials, in which ferroelectric and magnetic orders coexist, have been found. Many of them are antiferromagnets which have spin structures of spiral type, and their giant magnetoelectric effect has been attracting attention. Antiferromagnetic chromium oxide (Cr_2O_3 , Néel temperature $T_N = 307$ K) is not multiferroic, but has been interested in its magnetoelectric effect.

In the present study, we pay attention to the relation between spin and lattice in Cr_2O_3 and studied the optically induced lattice dynamics using the pump-probe technique. The pump pulse (0.2 ps, 1300 or 900 nm) and the probe pulse (0.2 ps, 800nm) are linearly polarized and collinear. The sample is excited by the pump pulse. The rotation of the polarization plane (rotation signal) and the ellipticity (ellipticity signal) of the transmitted probe pulse are measured.

The optically induced rotation signal for the pump of 1300 nm observed at 7 K shows a damped oscillation in the picosecond region. From its Fourier spectrum, it was found that the oscillation frequency is about 0.285 THz. When a magnetic field up to 5T was

applied, the oscillation frequency does not change. This shows that the observed damped oscillation is considered to be a lattice vibration.

The optically induced ellipticity signals for the pump of 900 nm decay exponentially in the nanosecond region. The signals were fitted using a single-exponential fitting function, and the relaxation time was obtained. In some temperature regions, the single-exponential fitting does not work. A double-exponential fitting function was used to fit the two components, and the slow and fast relaxation times were obtained.

It was found that the relaxation rate of the slow component diverges toward the antiferromagnetic transition temperature ($T_N = 307$ K). Generally, there is no correlation between the lattice and spin, but this behavior is considered to be a peculiar phenomenon to materials that have the electromagnetic effect in which spin and lattice are correlated. The relaxation rate of the fast component diverges around 200 K. This divergence behavior away from the Néel temperature is thought to be related to an activation energy process.

Electric-field induced magnetization in YIG observed by Faraday rotation

Y. Mushiaki¹, K. Fujimoto¹, T. Hasunuma¹, and T. Kohmoto^{1,2}

¹Graduate School of Science, Kobe University

²Molecular Photoscience Research Center, Kobe University

(*iCAMP 2020*)

Yttrium iron garnet (YIG, $\text{Y}_3\text{Fe}_5\text{O}_{12}$) is a ferrimagnetic material with a Curie temperature 560 K and is known to show a large Faraday effect. It has been reported that YIG shows a second-order magnetoelectric effect at room temperature and a first-order magnetoelectric

effect below 125 K. Furthermore, a second-order magnetoelectric effect at low temperatures was reported in the recent study.

In the present study, we observed the electric-field induced magnetization caused by the magnetoelectric effect in YIG (0.3 mm). The magnetization is detected as the Faraday rotation of a transmitted probe beam (1064 nm), using a polarimeter. In our experiment, the electric and magnetic fields were applied parallel to the direction of the probe beam.

The Faraday-rotation amplitude observed at 100 K has a linear dependence on the electric field in the

magnetic field of +1 T, which means the first-order magnetolectric effect at 100 K. While that observed at 225 K shows the first and second order magnetolectric effect. The observed Faraday-rotation amplitude S can be considered to be a sum of two components linear and quadratic in the electric field. We can define the fractions r_1 and r_2 of the first and second order effects for the electric field ($r_1 + r_2 = 1$). From the temperature dependence of the fraction r_1 and r_2 , it was found that, at lower temperatures, the first-order effect is dominant, and that the fraction r_2 of the second-order effect increases suddenly around 200 K.

Original Papers

発表論文

authors	title	journal	Vol.	page	year
Yasuhiro Kobori, Masaaki Fuki, Shunta Nakamura, Taku Hasobe	Geometries and Terahertz Motions Driving Quintet Multiexcitons and Ultimate Triplet-Triplet Dissociations via the Intramolecular Singlet-Fissions	<i>J. Phys. Chem. B</i>	124	9411–9419	2020.9.26
Yulian Han, Morihiko Hamada, I-Ya Chang, Kim Hyeon-Deuk, Yasuhiro Kobori, Yoichi Kobayashi	Fast T-Type Photochromism of Colloidal Cu-Doped ZnS Nanocrystals	<i>J. Am. Chem. Soc.</i>		doi.org/10.1021/jacs.0c10236	
Zhujun Zhang, Hiroki Nagashima, Takashi Tachikawa	Ultra-Narrow Depletion Layers in Hematite Mesocrystal-Based Photoanode for Boosting Multihole Water Oxidation	<i>Angewt. Chem. Int. Ed.</i>	59	9047-9054	2020.3.15
Izuru Karimata, Takashi Tachikawa	In Situ Exploration of the Structural Transition during Morphology- and Efficiency-Conserving Halide Exchange on a Single Perovskite Nanocrystal	<i>Angewt. Chem. Int. Ed.</i>	59	2548-2553	2020.10.19
Ji Young Hwang, Gun-hee Moon, Bupmo Kim, Takashi Tachikawa, Tetsuro Majima, Seungwoo Hong, Kangwoo Cho, Wooyul Kim, Wonyong Choi	Crystal phase-dependent generation of mobile OH radicals on TiO ₂ : Revisiting the photocatalytic oxidation mechanism of anatase and rutile	<i>Appl. Catal. B</i>	286	119905	2021.1.16
Naoya Haraguchi, Tomoki Okunaga, Yuto Shimoyama, Naoki Ogiwara, Soichi Kikkawa, Seiji Yamazoe, Miki Inada, Takashi Tachikawa, Sayaka Uchida	Formation of Mixed-Valence Luminescent Silver Clusters via Cation-Coupled Electron-Transfer in a Redox-Active Ionic Crystal Based on a Dawson-type Polyoxometalate with Closed Pores	<i>Eur. J. Inorg. Chem.</i>		in press	2021.3.18
Tatsuya Watase, Minoru Sohmiya, Zhujun Zhang, Yasuhiro Kobori, Takashi Tachikawa	Unraveling Hidden Correlations between Molecular Diffusivity and Reactivity in Ruthenium Complex-Modified Mesoporous Silica	<i>J. Phys. Chem. C</i>	124	21502-21511	2020.9.8
Kohei Tada and Shunji Kasahara	Hyperfine-resolved high-resolution laser spectroscopy interaction constants of ¹⁴ NO ₂ radical in 15885 cm ⁻¹ energy region	<i>J. Mol. Struct.</i>	1218	128529/1-9	2020.5.27
Kaoru Ohta, Yuichi Hiramatsu, Kohtarō Takahashi, Mitsuharu Suzuki, Hiroko Yamada, and Keisuke Tominaga	Dynamic Behavior of Photogenerated Charge Carriers in Diketopyrrolopyrrole-Linked Tetrabenzoporphyrin-Based Bulk Heterojunction Thin Films Probed with Time-Resolved Terahertz Spectroscopy	<i>J. Photochem. Photobiol. A: Chemistry</i>	400	112693	2020
Masaki Okuda, Takato Hiramatsu, Mitsuru Yasuda, Mika Ishigaki, Yukihiko Ozaki, Michitoshi Hayashi, Keisuke; Tominaga, and Eri Chatani	Theoretical Modeling for Electronic Structure of Polyiodide Species Included in α -Cyclodextrin	<i>J. Phys. Chem. B.</i>	124	4089-4096	2020.5.27
Norifumi Moritsugu, Takafumi Nara, Shin-ichi Koda, Keisuke Tominaga, and Shinji Saito	Molecular Mechanism of Acceleration and Retardation of Collective Orientation Relaxation of Water Molecules in Aqueous Solutions	<i>J. Phys. Chem. B.</i>	124	11730-11737	2020.12.15
Huiqiang Lu, Sergei G. Kazarian, Harumi Sato	Macromol Simultaneous Visualization of Phase Separation and Crystallization in PHB/PLLA Blends with In Situ ATR-FTIR Spectroscopic Imaging	<i>Macromolecules</i>	53	9074	2020.10.7

Tatsuro Nasu, Yukihiro Ozaki, Harumi Sato	Study of changes in water structure and interactions among water, CH ₂ , and COO ⁻ groups during water absorption in acrylic acid-based super absorbent polymers using Raman spectroscopy	<i>Spectrochimica Acta Part A</i>	250	119305	2020.12.11
Yumiko Yamamoto, Hiromichi Hoshina, Harumi Sato	Differences in Intermolecular Interactions and Flexibility between Poly(ethylene terephthalate) and Poly(butylene terephthalate) Studied by Far-Infrared/Terahertz and Low-Frequency Raman Spectroscopy	<i>Macromolecules</i>	54	1052	2021.1.7
Takashi Kunimoto, Yoshiko Fujita, Hiroshi Kajiyama, Tetsuo Honma, Hideki Kawaguchi, Tadashi Ishigaki, Koutoku Ohmi, Kentaro Ohshima, Daisuke Miyazaki, Yu Saito, Shigeo Hara, Takahiro Sakurai, Susumu Okubo, and Hitoshi Ohta	Development of Eu ²⁺ and Mn ²⁺ co-activated silicate phosphor for plant cultivation light source	<i>Jpn. J. Appl. Phys.</i>	58		2019.5
Eiichi MATSUOKA, Yasuo IWAKIRI, Akihiro OSHIMA, Hitoshi SUGAWARA, Takahiro SAKURAI, and Hitoshi OHTA	Magnetic and Transport Properties of New Cubic compounds Ce ₆ Pd ₁₃ Cd ₄ and R ₆ Pd ₁₃ Zn ₄ (R = Pr, Nd) with the Octahedral Rare-Earth Sublattices	<i>JPS Conf. Proc.</i>	30	011110/1-6	2019.9
Ryota SHIBUYA, Eiichi MATSUOKA, Hitoshi SUGAWARA, Takahiro SAKURAI, and Hitoshi OHTA	Magnetic, Transport, and Thermal Properties of New Cubic Compounds Ce ₆ Mg ₂₃ Z (Z = C, Si, Ge)	<i>JPS Conf. Proc.</i>	30	011109/1-5	2019.9
Takashi Uchino, Nanami Teramachi, Ryosuke Matsuzaki, Emi Tsushima, Shusuke Fujii, Yusuke Seto, Kazuyuki Takahashi, Takao Mori, Yutaka Adachi, Yukihiro Nagashima, Yoshifumi Sakaguchi, Kazuki Ohishi, Akihiro Koda, Takahiro Sakurai and Hitoshi Ohta	Proximity coupling of superconducting nanograins with fractal distributions	<i>Phys. Rev. B</i>	101	035146/1-12	2020.1
E. Ohmichi, T. Okamoto, T. Sakurai, H. Takahashi, S. Okubo, H. Ohta	Zero-Field Splitting Parameters of Hemin Investigated by High-Frequency and High-Pressure Electron Paramagnetic Resonance Spectroscopy	<i>Appl. Mag. Res. (Invited review)</i>	51	1103-1115	2020.8
A. Miyawaki, T. Mochida, T. Sakurai, H. Ohta, and K. Takahashi	The Impact of the Next-Nearest Neighbor Dispersion Interactions on Spin Crossover Transition Enthalpy Evidenced by Experimental and Computational Analyses of Neutral π -Extended Heteroleptic Fe(III) Complexes	<i>Inorganic Chemistry</i>	59	12295-12303	2020.8
J. Setsune, S. Omae, Y. Tsujimura, T. Mochida, T. Sakurai and H. Ohta	Synthesis, Structure, and Magnetic Properties of Linear Trinuclear CuII and NiII Complexes of Porphyrin Analogues Embedded with Binaphthol Units	<i>Symmetry</i>	12	1610/1-22	2020.9

E. Ohmichi, T. Okamoto, H. Takahashi, H. Ohta	Mechanically Detected Terahertz Electron Spin Resonance	<i>Appl. Mag. Res. (Invited review)</i>		in press	
Yoshiki Kuwata, Hisashi Kotegawa, Hideki Tou, Hisatomo Harima, Qing-Ping Ding, Keiki Takeda, Junichi Hayashi, Eiichi Matsuoka, Hitoshi Sugawara, Takahiro Sakurai, Hitoshi Ohta, and Yuji Furukawa	Nonmagnetic first-order phase transition in the nonsymmorphic NbCrP	<i>Phys. Rev. B</i>		in press	
T. Sakurai, B. Rubrecht, L. T. Corredor, R. Takehara, M. Yasutani, J. Zeisner, A. Alfonsov, S. Selter, S. Aswartham, A. U. B. Wolter, B. Büchner, H. Ohta, and V. Kataev	Pressure control of the magnetic anisotropy of the quasi-two-dimensional van der Waals ferromagnet Cr ₂ Ge ₂ Te ₆	<i>Phys. Rev. B</i>	103	024404/1-8	2021.1
H. Takahashi, Y. Ishikawa, T. Okamoto, D. Hachiya, K. Dono, K. Hayashi, T. Asano, S. Mitsudo, E. Ohmichi, and H. Ohta	Force detection of high-frequency electron spin resonance near room temperature using high-power millimeter-wave source gyrotron	<i>Appl. Phys. Lett.</i>	118	022407/1-5	2021.1
Ryo Ogawa, Tatsunori Okada, Hideyuki Takahashi, Fuyuki Nabeshima and Atsutaka Maeda	Microwave Hall effect measurement for materials in the skin depth region	<i>J. Appl. Phys.</i>	129	015102/1-14	2021.1

Invited Talks (domestic and international)

招待講演(国内および国際研究集会)

発表者氏名	開催時期	開催地	plenary or invite	学会名	講演題目
小堀康博 Y. Kobori	2020. 9.10	online	invite	Annual Meeting on Photochemistry 2020 at Online	JPA Award 2019 Award Lecture: Photon-to-Energy Conversion Mechanisms Revealed by Quantum Effects on Electron Spin Polarization
	2020. 12.12	online	invite	6th Kanto Area Spin Chemistry Meeting (KASC 6)	Conformation Changes in Intramolecular Multiexciton Spins
立川貴士 T. Tachikawa	2020. 12.3	オンライン	invite	第30回キャラクターゼーション講習会	単一分子・単一粒子蛍光顕微鏡を用いた光触媒反応のその場観測
	2020. 3.1	オンライン	invite	光機能材料研究会 第81回講演会	単一分子・単一粒子蛍光顕微鏡を用いた光触媒反応のその場観測
	2020. 3.20	オンライン	invite	日本化学会 第101春季年会 (2021)	Single-Particle Emission Imaging of Stimulus-Induced Structural Changes
富永圭介 K. Tominaga	2020. 12.9	Singapore (online)	invite	Asian Spectroscopy Conference	THz Molecular Science in Condensed Phases
	2021.3. 8-9	University of Fukui (online)	invite	8 th International Workshop on Far-Infrared Technologies (IW-FIRT 2021)	THz Molecular Science in Condensed Phases
張峰 F. Zhang	2020. 10.10	Beijing (online)	invite	SPIE Asian Photonics	Interpretation of THz Intensities of Molecular Crystals: the Role of Mixing between Intermolecular and Intramolecular Vibrations
	2020. 12.20	Kolkata, India (online)	invite	ICCAES 2020	Towards Establishing THz Vibrational Spectroscopy in Molecular Crystalline Systems
佐藤春実 H. Sato (人間発達環境学研究科)	2021.3. 8-9	University of Fukui (online)	invite	8 th International Workshop on Far-Infrared Technologies (IW-FIRT 2021)	Intermolecular hydrogen bonding of polymer by terahertz and low-frequency Raman spectroscopy
太田仁 H. Ohta	2020.9. 28-10.2	Kazan, Russia (On-site+Online)	invite	Modern Development of Magnetic Resonance 2020	Multi-extreme THz ESR: present and future
	2020.11. 8-13	Buffalo, USA (Online)	plenary	IRMMW-THz 2020	Recent Developments of Multi-Extreme THz ESR
高橋英幸 H. Takahashi	2021. 3. 8-9	University of Fukui (online)	invite	8 th International Workshop on Far-Infrared Technologies (IW-FIRT 2021)	Force-detected high frequency electron spin resonance at 154 GHz using high-power millimeter-wave source gyrotron
赤木暢 M. Akaki	2021. 3. 8-9	University of Fukui (online)	invite	8 th International Workshop on Far-Infrared Technologies (IW-FIRT 2021)	Pulsed high-field ESR in multiferroic åkermanite materials
櫻井敬博 T. Sakurai (研究基盤センター)	2021.3. 22-26	The Institute for Solid State Physics (online)	invite	International Workshop on Quantum Magnets in Extreme Conditions	Development of Multi-extreme THz ESR Systems and Its Application to Orthogonal Dimer Spin Substance SrCu ₂ (BO ₃) ₂

Presentation at conferences (international and domestic)

一般講演

発表者氏名	開催時期	開催地	oral or poster	学会名	講演題目
小堀康博 Y. Kobori	2020. 11.15	オンライン	oral	第 59 回電子スピサイエンス学会年会	分子内一重項分裂によるスピン相関三重項対生成に対する振電効果
張峰 F. Zhang	2020 11.10	Buffalo, USA (online)	oral	IRMMW-THz 2020	Interpretation of THz Intensities of Molecular Crystals: the Role of Mixing between Intermolecular and Intramolecular Vibrations
	2020. 11.12	Buffalo, USA (online)	Oral	IRMMW-THz 2020	Determination of the Fine Structure of a Halide Perovskite using High-resolution THz Spectroscopy and Solid-state Density Functional Theory
	2020.12. 8-10	Singapore (online)	poster	Asia Spectroscopy Conference	Determination of the Fine Structure of a Halide Perovskite using THz Spectroscopy
太田仁 H. Ohta	2020. 11.27	オンライン	Oral	第 4 回スピン系物理研究会	三角格子反強磁性体 CsFeCl ₃ における圧力誘起磁気相転移の観測
大久保晋 S. Okubo	2020.9. 8-11	オンライン	Oral	日本物理学会 2020 年 秋季大会	CsFeCl ₃ の圧力誘起磁気相の ESR による研究 III
	2020.10. 29-30	オンライン	Oral	第 29 回(2020 年度)日本赤外線学会研究発表会	三角格子反強磁性体 CsFeCl ₃ の圧力下テラヘルツ ESR による研究
	2020.11. 13-15	オンライン	Oral	第 59 回電子スピサイエンス学会年会	圧力下 ESR 測定によるスピンギャップ系 CsFeCl ₃ の圧力下誘起磁気相の研究
	2021. 1.29	オンライン	Oral	第 18 回赤外放射応用関連学会等年会	テラヘルツ電子スピン共鳴の低次元磁性体への応用
	2021.3. 12-15	オンライン	Oral	第 76 回日本物理学会年次大会	ダイマー系化合物 CoSeO ₃ ·2H ₂ O の高周波 ESR 測定 IV
高橋英幸	2020.9.7	オンライン	Oral	第七回西日本強磁場科学研究会	熱的な検出方法による高周波 ESR の高感度化
	2020.9. 8-11	オンライン	Oral	日本物理学会 2020 年 秋季大会	154GHz ジャイロトロンを用いた室温における力検出型 ESR
	2020.10 29-30	オンライン	Oral	第 29 回(2020 年度)日本赤外線学会研究発表会	154GHz ジャイロトロンを用いた力検出型高周波 ESR 測定
	2020.11 13-15	オンライン	Oral	第 59 回電子スピサイエンス学会年会	力検出法の角度回転高周波 ESR への応用
	2021. 3.10	オンライン	Oral	2020 年度福井大学遠赤外領域開発研究センター共同研究成果報告会	高強度テラヘルツ光源を使用した力検出型電子スピン共鳴分光
	2021.3. 12-15	オンライン	Oral	第 76 回日本物理学会年次大会	熱検出型高周波電子スピン共鳴法の開発
赤木暢	2020.9. 8-11	オンライン	Oral	日本物理学会 2020 年 秋季大会	CuFeO ₂ における圧力下電子スピン共鳴
	2020.11 .3-15	オンライン	Oral	第 59 回電子スピサイエンス学会年会	マルチフェロイック Sr ₂ CoSi ₂ O ₇ における ESR 方向二色性
河本敏郎 (理学研究科)	2020.7	奈良 (on line)	poster	International Conference on Condensed Matter Photo-Physics 2020	Spatial and temporal dynamics of thermal diffusion in clathrate compounds

	2020.9.8-11	熊本 (on line)	poster	日本物理学会 2020 年秋季大会	クラスレート化合物における熱拡散の空間的・時間的ダイナミクス: 格子拡散とキャリア拡散
櫻井敬博 (研究基盤センター)	2020.9.8-11	オンライン	Oral	日本物理学会 2020 年秋季大会	三角格子反強磁性体 CsCuCl ₃ の高圧下強磁場 ESRII
	2020.10.29-30	オンライン	Oral	第 29 回(2020 年度)日本赤外線学会研究発表会	圧力下サブミリ波 ESR 装置の開発と応用
	2020.11.13-15	オンライン	Oral	第 59 回電子スピンスイエンズ学会年会	高圧力下強磁場 ESR システムの開発と常磁性化合物 Co Tutton 塩への応用
	2020.12.1-3	オンライン	Oral	Asia-Pacific Conference on Research in High Magnetic Fields & KINKEN Materials Science School 2020 for Young Scientists	Development of high-pressure THz ESR system and its application to triangular lattice antiferromagnet CsCuCl ₃
	2021.3.12-15	オンライン	Poster	第 76 回日本物理学会年次大会	圧力下 THz ESR 装置における圧力較正手法の開発と応用
原茂生 (研究基盤センター)	2021.3.12-15	オンライン	Poster	第 76 回日本物理学会年次大会	ACo ₂ (SeO ₃) ₃ · 3(H ₂ O)(A=Sr, Ba) 単結晶育成の試みと光水熱合成炉の開発
齋藤佑 (研究基盤センター)	2020.11.13-15	オンライン	Oral	第 59 回電子スピンスイエンズ学会年会	極安定パーフルオロアルキルラジカルの低温 ESR 測定

Presentation by Graduate Students and Postdocs

院生、ポストドクの学会発表

指導教員	発表者氏名	学年	時期	学会名	講演題目
立川貴士 T.Tachikawa	田上嘉尉	M1	2020.3.21	日本化学会 第 101 春季 年会 (2021)	巨視的な自発分極を有する BiOIO ₃ における光 触媒反応の単一粒子蛍光観測
笠原俊二 S. Kasahara	清水暘	M1	2021.3. 9-10	5th Asian Workshop on Molecular Spectroscopy	Ultrahigh-resolution spectroscopy of trans- stilbene: nonplanar structure in the ground state
	中島康輔	M1	2021.3. 9-10	5th Asian Workshop on Molecular Spectroscopy	Ultrahigh-resolution Spectroscopy of acetaldehyde: Torsion-inversion-rotation interaction in the excited state
富永圭介 K.Tominaga	Lou Serafin Lozada	D2	2020.10. 19-23	38 th SPP Physics Conference (online)	Broadband dielectric relaxation of hydrated bentonite
	Lou Serafin Lozada	D2	2020.12. 8-10	7 th Asian Spectroscopy Conference 2020 (online)	Broadband dielectric spectroscopy from sub- GHz to THz frequency region on hydrated bentonite
	藤井 悠生	M2	2020.12. 8-10	7 th Asian Spectroscopy Conference 2020 (online)	Hydrogen Bond Dynamics of 9-Fluorenone Derivatives in Water Studied by Two- Dimensional Infrared Spectroscopy
	高本 和也	M1	2020.12. 8-10	7 th Asian Spectroscopy Conference 2020 (online)	Charge Transfer Dynamics of 9-Arylcarbazole Studied by Femtosecond Transient Absorption Spectroscopy
佐藤春実 H. Sato	西前 篤志	M2	2020.9.16	高分子討論会	テラヘルツおよび低波数ラマン分光法による PGAPLA 共重合体の組成比変化に伴う高次 構造の研究
	那須 達郎	M2	2020.9.16	高分子討論会	ラマン及び赤外スペクトルに現れる水と高吸水 性樹脂中の水の振動モードの比較
	能智 真央	M2	2020.9.16	高分子討論会	振動分光法を用いた ε ポリ(L)リジンの吸水に よる高次構造の研究
	西前 篤志	M2	2020.7.10	第 66 回高分子研究発表 会(神戸)	ポリ(グリコリド-ラクチド)共重合体の低波数領域 における振動モードの組成比依存性
	能智 真央	M2	2020.7.10	第 66 回高分子研究発表 会(神戸)	低波数領域の振動分光法を用いた ε ポリ(L)リ ジンの高次構造の研究
	那須 達郎	M2	2020.7.10	第 66 回高分子研究発表 会(神戸)	高吸水性樹脂中の水の振動モードの低波数領 域と高波数領域の比較
	吉江大成	M1	2020.7.10	第 66 回高分子研究発表 会(神戸)	生分解性ポリマーブレンドのテラヘルツイメー ジングによるモルフォロジー観察
	那須達郎	M2	2020.5.27	第 69 回高分子学会年次 大会	低波数ラマン分光法と赤外分光法によるアク リル酸系高吸水性樹脂中の水の構造
	吉江大成	M1	2020.5.27	第 69 回高分子学会年次 大会	THz イメージングによるポリヒドロキシブタン 酸/ポリ乳酸ブレンドの相分離
太田仁 H. Ohta	八谷大輝	M2	2020.9. 8-11	日本物理学会 2020 年 秋季大会	非反転対称磁性体 CuB ₂ O ₄ のテラヘルツ領域 における力検出型 ESR 分光
	恒石一義	M2	2020.9. 8-11	日本物理学会 2020 年 秋季大会	S=1/2 反強磁性鎖 KCuMoO ₄ (OH)の単結晶 ESR 測定 III
	船越風太	M2	2020.9. 8-11	日本物理学会 2020 年 秋季大会	ダイマー系化合物 CoSeO ₃ ·2H ₂ O の高周波 ESR 測定 III
	安谷佳将	M2	2020.9. 8-11	日本物理学会 2020 年 秋季大会	圧力下強磁場 ESR 装置における圧力校正手 法の開発 III

	船越風太	M2	2020.10.29-30	第 29 回(2020 年度)日本赤外線学会研究発表会	ダイマー系化合物 $\text{CoSeO}_3 \cdot 2\text{H}_2\text{O}$ のテラヘルツ波 ESR 測定
	藤岡廉	M2	2020.10.29-30	第 29 回(2020 年度)日本赤外線学会研究発表会	力検出型電子スピン共鳴測定の高感度向上に向けたテラヘルツ帯 bull's eye アンテナの作製
	八谷大輝	M2	2020.10.29-30	第 29 回(2020 年度)日本赤外線学会研究発表会	非反転対称磁性体 CuB_2O_4 の THz 領域における角度回転力検出型 ESR 測定
	恒石一義	M2	2020.10.29-30	第 29 回(2020 年度)日本赤外線学会研究発表会	S=1/2 反強磁性鎖 $\text{KCuMoO}_4(\text{OH})$ の微小単結晶試料を用いたテラヘルツ力検出 ESR 測定
	安谷佳将	M2	2020.10.29-30	第 29 回(2020 年度)日本赤外線学会研究発表会	多重極限 ESR 装置における圧力較正手法の確率と応用
	安谷佳将	M2	2020.11.13-15	第 59 回電子スピンサイエンス学会年会	多重極限 ESR 装置における圧力較正装置の開発と応用
	船越風太	M2	2020.11.13-15	第 59 回電子スピンサイエンス学会年会	スピンドイマー系化合物 $\text{CoSoO}_3 \cdot 2\text{H}_2\text{O}$ の高周波 ESR 測定
	恒石一義	M2	2020.11.13-15	第 59 回電子スピンサイエンス学会年会	S=1/2 反強磁性鎖 $\text{KCuMoO}_4(\text{OH})$ の微小単結晶試料を用いたメンブレン力検出 ESR 測定
	藤岡廉	M2	2020.11.13-15	第 59 回電子スピンサイエンス学会年会	力検出型 ESR 測定の高感度化に向けたテラヘルツ帯 bull's eye アンテナの作製と評価
	八谷大輝	M2	2020.11.13-15	第 59 回電子スピンサイエンス学会年会	非反転対称磁性体メタホウ酸銅のテラヘルツ領域における角度回転力検出型 ESR 分光
	竹原良祐	M1	2020.11.13-15	第 76 回日本物理学会年次大会	スピギャップ系物質の高圧下 THz ESR 測定
	小路悠斗	M1	2020.11.13-15	第 76 回日本物理学会年次大会	連続波長可変テラヘルツ光源を用いた周波数掃印型電子スピン共鳴分光法の開発
河本敏郎 T. Kohmoto	虫明侑一郎	M1	2020.7	International Conference on Condensed Matter Photo-Physics 2020	Electric-field induced magnetization in YIG observed by Faraday rotation
	岩崎祐典	M2	2020.7	International Conference on Condensed Matter Photo-Physics 2020	Terahertz time-domain spectroscopy in antiferromagnetic cobalt oxide
	前田悠貴	M2	2020.7	International Conference on Condensed Matter Photo-Physics 2020	Lattice dynamics in an antiferromagnet chromium oxide
	前田悠貴	M2	2020.9.8-11	日本物理学会 2020 年秋季大会	反強磁性体酸化クロムにおける高速格子ダイナミクス
	岩崎祐典	M2	2020.9.8-11	日本物理学会 2020 年秋季大会	反強磁性体酸化コバルトにおけるテラヘルツ時間領域分光
	虫明侑一郎	M1	2020.9.8-11	日本物理学会 2020 年秋季大会	YIG における電場誘起磁化
	岩崎祐典	M2	2020.10.26-28	日本分光学会年次講演会	遷移金属酸化物反強磁性体におけるテラヘルツ時間領域分光
	前田悠貴	M2	2020.10.26-28	日本分光学会年次講演会	反強磁性体 Cr_2O_3 における高速格子ダイナミクス
	虫明侑一郎	M1	2020.10.26-28	日本分光学会年次講演会	YIG における電場誘起磁化
	岩崎祐典	M2	2020.12.11-12	第 31 回光物性研究会	反強磁性体酸化コバルトにおけるテラヘルツ時間領域分光

前田悠貴	M2	2020.12. 11-12	第 31 回光物性研究会	反強磁性体酸化クロムにおける高速格子ダイナミクス
虫明侑一郎	M1	2020.12. 11-12	第 31 回光物性研究会	YIG における電場誘起磁化と光励起キャリアの拡散ダイナミクス

Books**著書**

著者（共著者も含む）	書名	出版社名	ページ数	発行年
------------	----	------	------	-----

Other Publications

参考論文・記事・報告

著者	タイトル	出版物名	巻・号・ページ	発行年
立川貴士	太陽光水素製造へ向けたヘマタイトメソ結晶光電極の開発	FC レポート	38 巻・4 号	2020
立川貴士	ヘマタイトメソ結晶光電極を用いた太陽光水素製造	月刊機能材料	40 巻・8 号	2020
立川貴士	赤錆を用いて水と太陽光から水素を製造	クリーンエネルギー	29 巻・3 号・37-42	2020
Carlos R. Baiz, Bartosz Błasiak, Jens Bredenbeck, Minhaeng Cho, Jun-Ho Choi, Steven A. Corcelli, Arend G. Dijkstra, Chi-Jui Feng, Sean Garrett-Roe, Nien-Hui Ge, Magnus W. D. Hanson-Heine, Jonathan D. Hirst, Thomas L. C. Jansen, Kijeong Kwac, Kevin J. Kubarych, Casey H. Londergan, Hiroaki Maekawa, Mike Reppert, Shinji Saito, Santanu Roy, James L. Skinner, Gerhard Stock, John E. Straub, Megan C. Thielges, Keisuke Tominaga, Andrei Tokmakoff, Hajime Torii, Lu Wang, Lauren J. Webb, and Martin T. Zanni	Vibrational Spectroscopic Map, Vibrational Spectroscopy, and Intermolecular Interaction	<i>Chem. Rev.</i>	120 (15) 7152-7218	2020
岩崎祐典, 喜多将之, 爰川優太, 守安毅, 河本敏郎	反強磁性体酸化コバルトにおけるテラヘルツ時間領域分光	光物性研究会論文集	31 巻・45-48	2020
前田悠貴, 川畑将馬, 三井宏務, 谷口弘樹, 疋田峻, 河本敏郎	反強磁性体酸化クロムにおける高速格子ダイナミクス	光物性研究会論文集	31 巻・141-144	2020
虫明侑一郎, 永富寛弥, 藤本恵輔, 河本敏郎	YIG における電場誘起磁化と光励起キャリアの拡散ダイナミクス	光物性研究会論文集	31 巻・257-260	2020

Lecture to Public

講演、模擬授業など

氏名	講演題目	集会名	日時	場所
小堀康博	電子スピンの量子・動的効果で読み解く光エネルギー変換のしくみ	“光”機到来！Qコロキウム	2020.12.2	https://www.youtube.com/watch?v=2Thnnebljnk
笠原俊二	温室効果ガスってなに？	第15回女子中高生のための関西科学塾	2021.3.20	神戸大学(オンライン)

Awards

受賞

氏名	受賞研究題目	賞名	団体、学会名
藤井悠生	Hydrogen Bond Dynamics of 9-Fluorenone Derivatives in Water Studied by Two-Dimensional Infrared Spectroscopy	IAS-Laser 21 Poster Award at Asian Spectroscopy Conference 2020	Asian Spectroscopy Conference 2020
八谷大輝	非反転対称磁性体 CuB_2O_4 の THz 領域における角度回転力検出型 ESR 測定	第 29 回 (令和 2 年度) 優秀発表賞	日本赤外線学会
安谷佳将	多重極限 ESR 装置における圧力較正手法の確立と応用	第 29 回 (令和 2 年度) 優秀発表賞	日本赤外線学会
安谷佳将	圧力較正装置を備えた新しい多重極限 ESR 装置の開発と応用	優秀発表賞	修士論文審査会 (2021 年 3 月)

Conference Organization

学術集会の開催

氏名	学術集会	共同主催者	場所	時期	参加者概数
立川貴士	先端融合研究環 開拓プロジェクト「階層縦断的アプローチによる革新的光エネルギー変換系の開拓」ワークショップ ~マテリアルサイエンスの最前線~		瀧川記念学術交流会館大会議室+online	2020.11.10	59名
笠原俊二、馬場正昭、富永圭介	テラヘルツ分子科学研究会「高分解能分光の最近の進展と今後の展望~テラヘルツ波とのinterplay」		神戸大学百年記念館+online	2020.12.3	約20名
笠原俊二	第21回分子分光研究会	石川春樹、水瀬賢太	Online	2021.3.8	約60名
笠原俊二、馬場正昭	5 th Asian Workshop on Molecular Spectroscopy	Thomas Schultz, Yen-Chu Hsu, Shuiming Hu	瀧川記念学術交流会館大会議室+online	2021.3.9-10	約100名
太田仁、大久保晋	分子フォト研究会「第4回スピン系物理研究会 スピン系研究の開拓前線」		online	2020.11.27	約50名
太田仁、大久保晋	第15回量子スピン系研究会		online	2021.1.5	36名

Seminars

セミナー

Date	Name	Affiliation	Title
2020.12.14	松本 正茂	静岡大学理学部	三角格子反強磁性体 CsFeCl ₃ における磁気励起
2021.3.11	今堀 博	京都大学大学院工学研究科 分子工学専攻	光電荷分離工学：モデル系から光エネルギー変換、細胞操作まで

Molecular Photoscience Research Center
Kobe University,
Nada, Kobe 657-8501 Japan

Tel: +81-78-803-5761

URL: http://www.research.kobe-u.ac.jp/mprc/about/index_e.html (English)

〒657-8501
神戸市灘区六甲台町 1-1
神戸大学分子フォトサイエンス研究センター

電話番号 078-803-5761

<http://www.research.kobe-u.ac.jp/mprc/index.html> (日本語)